

Sensitivity- and Uncertainty-Based Criticality Safety Validation Techniques

B. L. Broadhead, B. T. Rearden,* and C. M. Hopper

*Oak Ridge National Laboratory
P.O. Box 2008, Oak Ridge, Tennessee 37831-6370*

J. J. Wagschal

*The Hebrew University of Jerusalem
Racah Institute of Physics, 91904, Jerusalem, Israel*

and

C. V. Parks

*Oak Ridge National Laboratory
P.O. Box 2008, Oak Ridge, Tennessee 37831-6370*

Received January 9, 2003

Accepted June 20, 2003

Abstract—*The theoretical basis for the application of sensitivity and uncertainty (S/U) analysis methods to the validation of benchmark data sets for use in criticality safety applications is developed. Sensitivity analyses produce energy-dependent sensitivity coefficients that give the relative change in the system multiplication factor k_{eff} value as a function of relative changes in the cross-section data by isotope, reaction, and energy. Integral indices are then developed that utilize the sensitivity information to quantify similarities between pairs of systems, typically a benchmark experiment and design system. Uncertainty analyses provide an estimate of the uncertainties in the calculated values of the system k_{eff} due to cross-section uncertainties, as well as correlation in the k_{eff} uncertainties between systems. These uncertainty correlations provide an additional measure of system similarity. The use of the similarity measures from both S/U analyses in the formal determination of areas of applicability for benchmark experiments is developed. Furthermore, the use of these similarity measures as a trending parameter for the estimation of the computational bias and uncertainty is explored. The S/U analysis results, along with the calculated and measured k_{eff} values and estimates of uncertainties in the measurements, were used in this work to demonstrate application of the generalized linear-least-squares methodology (GLLSM) to data validation for criticality safety studies.*

An illustrative example is used to demonstrate the application of these S/U analysis procedures to actual criticality safety problems. Computational biases, uncertainties, and the upper subcritical limit for the example applications are determined with the new methods and compared to those obtained through traditional criticality safety analysis validation techniques.

The GLLSM procedure is also applied to determine cutoff values for the similarity indices such that applicability of a benchmark experiment to a criticality safety design system can be assured. Additionally, the GLLSM procedure is used to determine how many applicable benchmark experiments exceeding a certain degree of similarity are necessary for an accurate assessment of the computational bias.

*E-mail: reardenb@ornl.gov

I. INTRODUCTION

The American national standard for nuclear criticality safety in operations with fissionable material outside reactors, ANSI/ANS-8.1-1998 (Ref. 1), allows the use of calculations in the determination of subcritical limits for the design of fissionable material systems. The standard requires validation of the analytical methods and data used in nuclear criticality safety calculations in order to quantify any computational bias and the uncertainty in the bias. The validation procedure must be conducted through comparison of the computed results with experimental data, and the design system for which the subcritical limit is established must fall within the area of applicability of the experiments chosen for validation. The standard defines the area (or areas) of applicability as “the limiting ranges of material compositions, geometric arrangements, neutron energy spectra, and other relevant parameters (e.g., heterogeneity, leakage, interaction, absorption, etc.) within which the bias of a computational method is established.” For design systems that fall outside the area of applicability of available experiments, the standard allows for the use of trends in the bias to extend the range of the experimental conditions. The standard further states, “Where the extension is large, the method should be supplemented by other computational methods to provide a better estimate of the bias, and especially its uncertainty in the extended area (or areas), and to demonstrate consistency of computed results.” The standard provides no guidance with respect to the determination of what constitutes a valid area of applicability, under what conditions a given system is considered to fall outside an area of applicability, or when any extension outside the area of applicability is considered to be large.

In compliance with the standards, the nuclear criticality safety community in the United States typically evaluates the computational biases and uncertainties of its computational methods and nuclear data through the use of trending analyses. For a traditional trending analysis, a suite of critical-experimental benchmarks is selected with physical characteristics that are similar to the corresponding values in the design system for which the subcritical limit is to be established.² Some physical characteristics used to evaluate system similarity are fissile element(s), fissile concentration, moderator type, geometrical configuration, hydrogen-to-fissile atom ratios (H/X), average neutron-energy group causing fission, and energy of average neutron lethargy causing fission (EALF). Typically, the trending parameters are calculated as averages over the entire benchmark experiment.

Each of the experiments in the benchmark suite is modeled with the same code and data that will be used in the criticality safety analysis of the design system. The difference between the measured and calculated value of the effective neutron multiplication factor k_{eff} of a critical experiment is considered to be the computational bias

for that experiment. The expected computational bias of the design system is established through a trending analysis of the bias for all of the selected critical experiments as a function of their physical characteristics (e.g., H/X, EALF, etc.). The uncertainty in the bias is established through a statistical analysis of the trend.

With the use of traditional validation techniques, the establishment of the area of applicability and selection of a trending parameter is limited to the engineering judgment of the criticality safety analysts,³ who have estimated that the actual critical conditions of the design system can be computationally predicted within the limits of the bias and uncertainty established using the benchmarks. For design systems that have few or no benchmark experiments with similar physical characteristics, it is difficult, even through expert judgment, to assess the coverage of the system within the area of applicability of the available experiments. Some examples of systems for which limited applicable benchmark experiments are available include

1. intervening materials and configurations used in the packaging of unirradiated and irradiated fissionable materials for transport and storage
2. fissionable material operations involving neutron interaction between high-neutron-leakage fissionable material units
3. neutron reflector influences on large systems of heterogeneous fissionable material units (e.g., packaged waste and weapon components or reactor fuel)
4. operations involving mixed weapons-grade plutonium and uranium oxides with varying degrees of neutron moderation
5. operations involving fissionable materials that have a predominance of fission chains initiated with intermediate neutron energies such as systems of damp oxides of low-enriched to moderately enriched damp uranium, damp oxides of plutonium or ^{233}U , systems using large quantities of thermal $1/v$ or resonance neutron absorbers
6. irradiated and spent-fuel configurations in transport and storage.

Because of increasing costs to perform experimental measurements, the reliance on computational methods has increased. For the example systems mentioned earlier, and others, the applicability of available benchmark experiments to perform criticality validations is suspect. A more formal procedure is needed to assist in the definition of the area of applicability such that the similarity of experiments and design systems is quantifiable and less reliant on varied judgments. For design systems that extend beyond the area of applicability, especially where the extension is large, a method for predicting the computational bias and its uncertainty is needed.

With the joint support of the U.S. Nuclear Regulatory Commission and the U.S. Department of Energy's Nuclear Criticality Safety Program, Oak Ridge National Laboratory (ORNL) has been working to

1. devise a rigorous physics-based approach for the determination of system similarity, which can be used to assess coverage of a design system within the area of applicability of critical experiments
2. formulate the methodology and approach needed for determination of the computational biases and uncertainties due to experimental descriptions, computational methods, and nuclear data
3. develop the software tools needed to implement the methodology
4. provide illustrations and example guidance for the applications of these biases and uncertainties for defensible margins of subcriticality and safety.

To achieve these goals, prototypic sensitivity and uncertainty (S/U) analysis methods have been designed for use within the Standardized Computer Analyses for Licensing Evaluation (SCALE) code system.⁴⁻⁶ The basis of these analysis techniques is that systems with neutron multiplication factors that exhibit similar sensitivities to perturbations in the neutron cross-section data on an energy-dependent, nuclide-reaction specific level will have similar biases due to the computational method and nuclear data used in the criticality safety analysis. To quantify the similarity between a particular experiment and a design system, two types of integral indices were derived. Each of these integral indices consists of a bounded single value that determines whether or not the design system falls within the area of applicability of a given experiment. The first integral index E_{sum} is based only on sensitivity data and gives a measure of the commonality of the k_{eff} response of an experiment and a design system to perturbations in the cross-section data. The second integral index c_k couples the sensitivity data with tabulated cross-section-covariance data to give a correlation coefficient that provides a measure of the shared variance, due to cross-section uncertainties, in the computed value of k_{eff} for the design system and a given experiment. Each of these integral indices can be used in advanced trending studies to predict the computational bias and its uncertainty as a function of system similarity. Independently, but in comparison with the integral indices, an implementation of generalized linear-least-squares methodology (GLLSM) rigorously predicts the computation bias of a design system based on the sensitivity, cross-section-covariance, and experimental uncertainty data.

This paper provides the theoretical development of each of these tools and provides example applications and guidance for their use.

II. TRADITIONAL TRENDING ANALYSIS

Before formally introducing the S/U techniques for criticality safety analysis validation, a review of a representative traditional trending technique commonly used by criticality practitioners is presented. Where analytical methods are used to predict the criticality condition of a design system, the American National Standard ANSI/ANS-8.17-1984 (R1997) (Ref. 7) requires that the calculated multiplication factor k_s shall not exceed a maximum allowable value established as

$$k_s \leq k_c - \Delta k_s - \Delta k_c - \Delta k_m, \quad (1)$$

where

k_s = the calculated allowable maximum multiplication factor k_{eff} of the system being evaluated for normal or credible abnormal conditions or events;

k_c = the mean k_{eff} that results from the calculation of the benchmark criticality experiments using a particular computational method. If the calculated k_{eff} values for the criticality experiments exhibit a trend with a parameter, then k_c shall be determined by extrapolation on the basis of a best fit to the calculated values. The criticality experiments used as benchmarks in computing k_c should have physical compositions, configurations, and nuclear characteristics (including reflectors) similar to those of the system being evaluated;

Δk_s = an allowance for

- (a) statistical or convergence uncertainties, or both in the computation of k_s ;
- (b) material and fabrication tolerances;
- (c) uncertainties due to limitations in the geometric or material representations used in the computational method;

Δk_c = a margin for uncertainty in k_c which includes allowance for

- (a) uncertainties in the critical experiments;
- (b) statistical or convergence uncertainties, or both, in the computation of k_c ;
- (c) uncertainties due to extrapolation of k_c outside the range of experimental data;
- (d) uncertainties due to limitations in the geometrical or material representations used in the computational method

Δk_m = an arbitrary margin to ensure the subcriticality of k_s .

Consistent with the requirements of ANSI/ANS-8.17-1984 (R1997), a criticality code is typically validated against a suite of critical experiments to define an upper subcritical limit (USL) for design systems. According to the standard, the computed k_{eff} value of a design system (i.e., k_s) should not exceed the maximum acceptable value. This is expressed as

$$k_s + 2\sigma \leq USL = 1.00 + \beta - \Delta\beta - \Delta k_m, \quad (2)$$

where σ is the standard deviation of the computed value k_s ; β and $\Delta\beta$ represent the computational bias and uncertainty in the bias, respectively.⁸ For critical experiments, the computational bias is the difference between the mean value of k_{eff} calculated for the critical experiments k_c and 1.0 (i.e., $\beta = k_c - 1.0$). In practice, certain critical experiments may exhibit calculated k_{eff} values >1.0 , leading to a positive bias and reducing the required subcritical margin for the design system. However, regulatory impositions typically have not allowed for a positive computational bias; thus, β is either negative or zero. The quantity Δk_m is often referred to as an administrative margin and commonly assigned a value between 2 and 5% in k_{eff} (e.g., $\Delta k_m = 0.05$), depending on the application and regulatory guidance.

Two commonly used approaches for the calculation of the USL based on a suite of criticality experiments covering a particular area of applicability are (a) confidence band with administrative margin, referred to as USL_1 , and (b) single-sided uniform-width closed-interval approach, also called the lower tolerance band (LTB) method, and referred to as USL_2 (Ref. 2). The statistical analysis used in the computation of USL_1 and USL_2 is valid only within the range of applicability of the chosen trending parameter. The range of applicability is the portion of the area of applicability pertaining to the single selected trending parameter. Any extrapolation outside the range of applicability requires a different statistical treatment. The USL obtained with the first method as a function of some trending parameter t is defined as

$$USL_1(t) = 1.0 - \Delta k_m - W + \beta(t). \quad (3)$$

The confidence bandwidth W provides a statistical estimate for the uncertainty in the bias $\Delta\beta$, which accounts for uncertainties in the experiments, computational method, and data. The maximum value is W , evaluated at the endpoints of the range of applicability of a confidence band $w(t)$, which is based on a statistically specified confidence level $(1 - \gamma_1)$, and the calculated k_{eff} values for the critical experiments. The lower confidence limit, which is $k_c(t) - W$, provides a $(1 - \gamma_1)$ confidence that the calculated k_{eff} values for the critical experiments are above the lower confidence limit. The confidence band is directly proportional to the standard deviation in the data and the specified level of confidence. A higher confidence level or larger standard deviation will lead to a larger value of W .

The USL_1 approach is illustrated in Fig. 1 where the computed values of k_{eff} are trended against some generic parameter. In Fig. 1 the computed k_{eff} values for 12 critical experiments are shown with their associated uncertainties as error bars. The solid line depicts $k_c(t)$, the linear regression fit to the computed data. Curves representing $k_c(t) - w(t)$, $k_c(t) - W$, and USL_1 are also shown. Because of the disallowance of positive biases, the USL_1 curve has a constant value where $k_c(t)$ exceeds 1.0. The positive bias adjustment in $k_c(t) - W$ is noted in Fig. 1. To evaluate the USL for a design application, using this approach, the value of the trending parameter for the design application would be assessed, and the USL_1 k_{eff} value would be read from Fig. 1. Then, because W is computed only within the range of applicability, the statistical approach used in the calculation USL_1 does not allow for extrapolation outside of the range of applicability of the chosen trending parameter. If extrapolations are required, the value of $w(t)$ should be evaluated in place of W .

In the LTB method, statistical techniques are used to determine a combined LTB plus administrative margin Δk_m . The USL obtained with this method is defined as

$$USL_2(t) = 1.0 - (C_{\alpha/\rho} \cdot s_\rho) + \beta(t), \quad (4)$$

where s_ρ is the pooled variance for the linear fit to the data $k_c(t)$; $C_{\alpha/\rho}$ is a statistically determined multiplier for a specified confidence α and probability ρ . The term $C_{\alpha/\rho} \cdot s_\rho$ provides an LTB such that there is α confidence and ρ probability that a future criticality calculation of a design system will lie above the LTB. The term $C_{\alpha/\rho} \cdot s_\rho$ can also be used to provide a statistical estimate of the administrative subcritical margin Δk_m . Moreover, Δk_m is

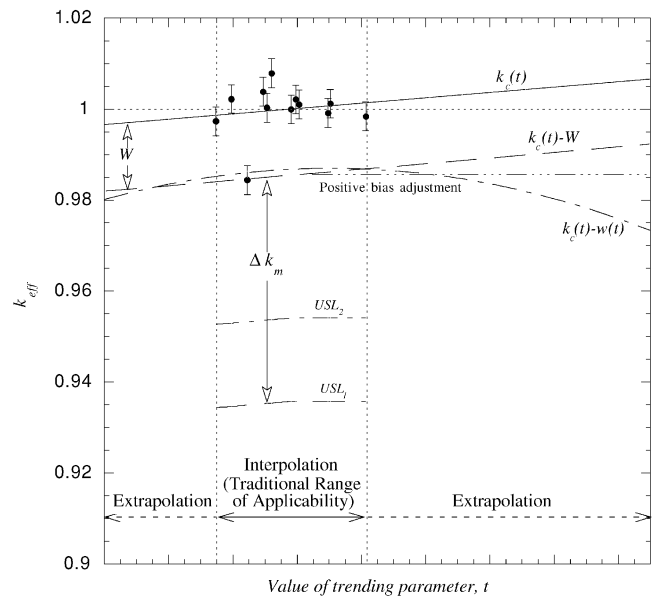


Fig. 1. Example trending analysis diagram.

the difference between $C_{\alpha/\rho} \cdot s_\rho$ and the confidence band W (i.e., $\Delta k_m = C_{\alpha/\rho} \cdot s_\rho - W$). Both USL_1 and USL_2 values are computed by the USLSTATS computer code.² Example uses of the traditional trending methodologies are presented in Sec. VII.B.

III. SENSITIVITY ANALYSIS TECHNIQUES

As an alternative to the traditional system-averaged trending parameters, ORNL has utilized sensitivity techniques to provide a quantifiable physics-based measure of the similarity of a design system and an experiment. The similarity measure can be used to determine whether or not a design system falls within the area of applicability of an experiment. With the sensitivity methods, the similarity measure is based on the energy-dependent, nuclide-reaction specific sensitivity of k_{eff} to the cross-section data. Based on the sensitivity, where a design system exhibits a certain degree of similarity to the experiment, the design system is deemed to fall within the area of applicability of the experiment.

III.A. Sensitivity Theory

Sensitivity coefficients are defined physically such that they represent the percentage effect on some system response due to a percentage change in an input parameter. For fissionable material systems, one of the appropriate responses is the system multiplication factor k_{eff} . The sensitivity coefficients are typically presented as profiles, where the change in k_{eff} due to perturbations of the cross-section data is given as a function of cross-section energy. These sensitivity profiles can be generated for each material in the system and may include various nuclear reactions (e.g., scatter, absorption, fission) as well as the neutron energy distribution from fission χ and average number of neutrons emitted per fission $\bar{\nu}$.

In this work, the sensitivity coefficients are calculated using the well-established adjoint-based perturbation theory approach.⁹⁻¹³ The full derivation of the general procedure is not given here; however, the specific theory for the generation of k_{eff} sensitivities is presented below. For the full derivation of the general sensitivity equations, the reader is referred to Ref. 13.

The Boltzmann transport equation is written in the form

$$[A - \lambda B]\phi = 0, \quad (5)$$

where A and B are loss and production operators, ϕ is the angular neutron flux, and λ represents the eigenvalues where the largest eigenvalue is $1/k_{eff}$. Define perturbed transport operators and the perturbed eigenvalues as

$$\begin{aligned} A' &= A + \delta A, \\ B' &= B + \delta B, \end{aligned}$$

and

$$\lambda' = \lambda + \delta\lambda, \quad (6)$$

where δA and δB represent small linear perturbations in their corresponding transport operators and $\delta\lambda$ represents the resulting change in the eigenvalues. The perturbed transport equation can be written in the form

$$[A' - \lambda' B']\phi' = 0. \quad (7)$$

The equation adjoint to Eq. (5) is

$$[A^* - \lambda B^*]\phi^* = 0, \quad (8)$$

where ϕ^* is the adjoint flux, also known as the importance function, and A^* and B^* are the adjoint operators corresponding to A and B .

Multiplying Eq. (7) by ϕ^* , and integrating over all phase-space, yields

$$\langle \phi^*(A' - \lambda' B')\phi' \rangle = 0, \quad (9)$$

where $\langle \rangle$ represents integration over all phase-space (volume, energy, and direction).

Expanding Eq. (9) in terms of Eq. (6) yields

$$\langle \phi^*(A - \lambda B + \delta A - \lambda \delta B - B \delta \lambda - \delta \lambda \delta B)\phi' \rangle = 0. \quad (10)$$

Using the property of adjointness (i.e., $\langle \phi^*(A - \lambda B)\phi' \rangle = \langle \phi'(A^* - \lambda B^*)\phi^* \rangle$) and Eq. (8) to reduce the number of terms yields

$$\langle \phi^*(\delta A - \lambda \delta B - B \delta \lambda - \delta \lambda \delta B)\phi' \rangle = 0. \quad (11)$$

Equation (11) is further simplified by ignoring the second-order perturbation term ($\delta \lambda \delta B$) and substituting ϕ' with ϕ , indicating that the perturbations in the transport operators do not cause significant perturbations in the flux solution. The eigenvalue perturbation becomes

$$\frac{\delta\lambda}{\lambda} = \frac{\langle \phi^*(\delta A - \lambda \delta B)\phi \rangle}{\langle \phi^*(\lambda B)\phi \rangle}. \quad (12)$$

Substituting the perturbation terms with partial derivatives with respect to a particular nuclide-reaction pair cross section Σ_x , the relative sensitivity of λ becomes

$$\frac{\Sigma_x}{\lambda} \frac{\partial\lambda}{\partial\Sigma_x} = \frac{\Sigma_x}{\lambda} \frac{\left\langle \phi^* \left(\frac{\partial A}{\partial\Sigma_x} - \lambda \frac{\partial B}{\partial\Sigma_x} \right) \phi \right\rangle}{\langle \phi^* B \phi \rangle}. \quad (13)$$

Note that since $\lambda = 1/k_{eff}$, then $\partial\lambda/\lambda = -\partial k_{eff}/k_{eff}$ such that the sensitivity of k_{eff} to some macroscopic cross section Σ_x is defined as

$$S_{k,\Sigma_x} = \frac{\Sigma_x}{k_{eff}} \frac{\partial k_{eff}}{\partial \Sigma_x} = -\frac{\Sigma_x}{\lambda} \frac{\partial \lambda}{\partial \Sigma_x} = -\frac{\Sigma_x}{k_{eff}} \frac{\left\langle \phi^* \left(\frac{\partial A}{\partial \Sigma_x} - \frac{1}{k_{eff}} \frac{\partial B}{\partial \Sigma_x} \right) \phi \right\rangle}{\left\langle \phi^* \frac{B}{k_{eff}^2} \phi \right\rangle}. \quad (14)$$

In practice, the $\partial A/\partial \Sigma_x$ and $\partial B/\partial \Sigma_x$ terms in Eq. (14) are simple functions of the scattering, capture, and fission cross-section data. The evaluation of Eq. (14) then becomes an integration of the forward and adjoint fluxes and the cross sections over the entire phase-space.

Typically, the energy dependence of the cross-section data is represented by averaging the Σ_x quantities over an energy group g and is represented as $\Sigma_{x,g}$. Insertion of these group quantities into Eq. (14) yields the sensitivity of k_{eff} to perturbations in a single energy group of a particular nuclear-reaction pair as

$$S_{k,\Sigma_{x,g}} = \frac{\Sigma_{x,g}}{k_{eff}} \frac{\partial k_{eff}}{\partial \Sigma_{x,g}}. \quad (15)$$

When g is varied to obtain the sensitivity for all groups, which span the energy range of interest, an energy-dependent sensitivity profile is generated.

The implementation of first-order adjoint-based sensitivity analysis used to develop Eq. (14) is consistent with that developed for and used previously in the FORSS code system at ORNL (Ref. 13). However, it has been demonstrated that this methodology is incomplete and only accounts for the explicit effect due to the perturbation of the macroscopic cross-section data components in the criticality calculation.¹⁴ The sensitivity coefficients as computed in Eq. (15) require another term to account for the first-order implicit effect of perturbations in the material number densities or nuclear data upon the shielded groupwise macroscopic cross-section data. The implicit portion of the sensitivity coefficient is defined as

$$S_{\Sigma_{x,g},\omega_i} = \frac{\omega_i}{\Sigma_{g,x}} \frac{\partial \Sigma_{x,g}}{\partial \omega_i}, \quad (16)$$

where ω_i is the number density of a particular material or a certain nuclear data component. The sensitivity coefficients defined in Eq. (16) can be propagated to the k_{eff} sensitivity via the chain rule for derivatives. Where the implicit sensitivity is added to the explicit sensitivity, the complete sensitivity coefficient, accounting for both the explicit and implicit terms, can be presented as

$$(S_{k,\Sigma_{x,g}})_{tot} = S_{k,\Sigma_{x,g}} + \sum_i \sum_y \sum_h S_{k,\Sigma_{y,h}} S_{\Sigma_{y,h},\omega_i} S_{\omega_i,\Sigma_{x,g}}, \quad (17)$$

where i is summed over all parameters that are dependent on the groupwise cross section $\Sigma_{x,g}$ and y and h are summed over all nuclide-reaction pairs and energy groups that are dependent on ω_i . The implementation of this methodology is explained in more detail in a companion paper.⁶

As examples, sensitivity profiles for ²³⁵U fission for three critical systems are shown in Fig. 2. Each of these systems is from the LEU-COMP-THERM-032 series of experiments from the *International Handbook of Evaluated Criticality Safety Benchmark Experiments*¹⁵ (IHECSBE). This series of experiments consists of water-flooded lattices of UO₂ fuel pins enriched to 10 wt% in ²³⁵U. The first two sensitivity profiles shown in Fig. 2 are for tightly packed lattices at 20 and 166°C, respectively. The third sensitivity profile shown in Fig. 2 is for the seventh core detailed in the experiment evaluation, a loosely packed lattice at 20°C.

As depicted in Fig. 2, the energy-dependent response of k_{eff} to perturbations in the ²³⁵U fission cross-section data for the first system is similar to that of the second system. The shape and magnitude of the profile for the third system are different from those of the first system. Had the first profile been generated for a design system and the second and third profiles for benchmark experiments, the second system would exhibit more similarities to the first than does the third. Thus, the second system would be more applicable to the criticality code validation of the first system. Sensitivity profiles could be generated to compare the response of each of these systems to perturbations of other nuclide-reaction pairs to provide a complete analysis of system similarity and demonstrate the ability of the benchmark experiment to validate the particular reaction over the energy range. Although it is instructive to assess similarity by visually comparing the sensitivity profiles of one system to those of another, the effort required to use such a manual procedure in a production environment is prohibitive. Furthermore, the establishment of a consistent quantitative measure of system similarity would be difficult.

III.B. Sensitivity-Based Integral Indices

In order to automate the process of assessing system similarity based on the sensitivity profiles, the development of a number of different sensitivity-based integral indices has been studied in this work.¹⁶ The objective is to produce a single index that quantifies the similarity between two systems, such that this single index could be used for the determination of applicability and as a trending parameter.

Initially, parameters using the absolute value of the sensitivity differences by group were developed. These “D” values are defined as

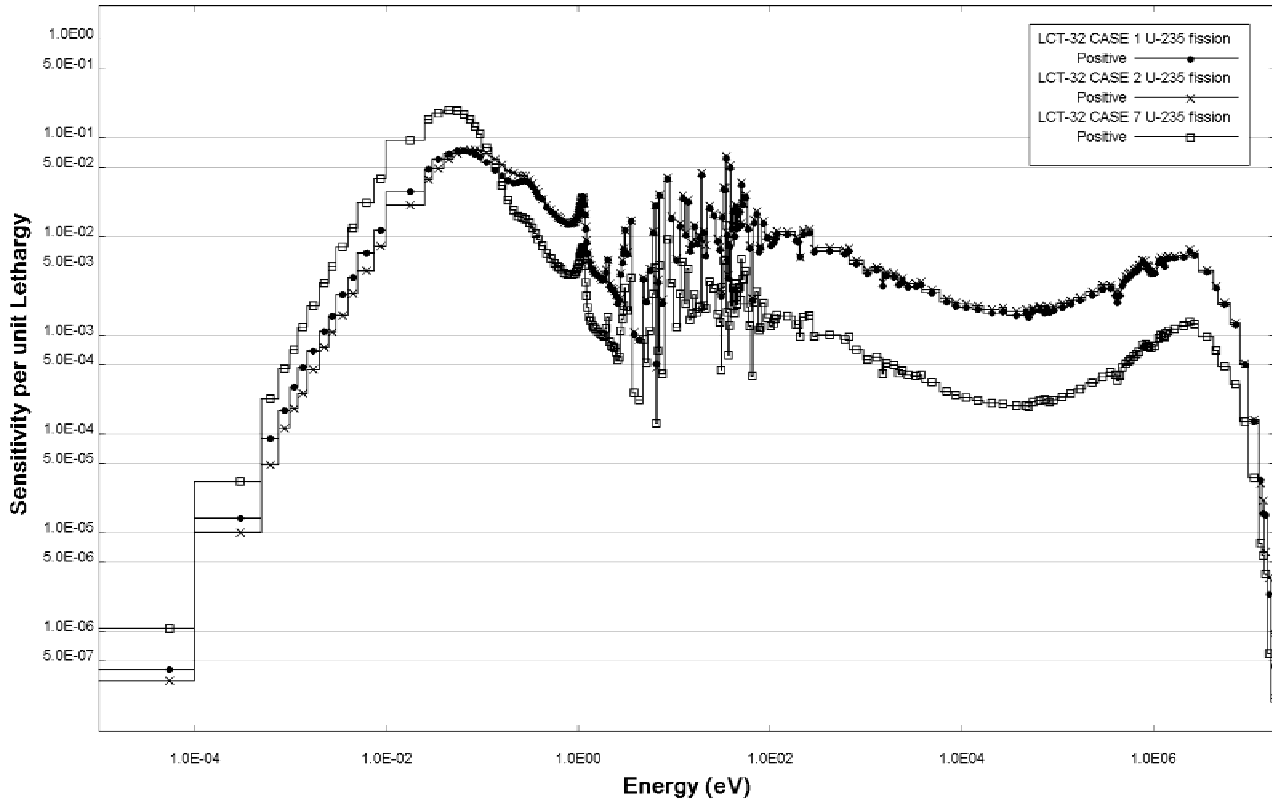


Fig. 2. The ^{235}U fission sensitivity profiles for LEU-COMP-THERM-032 cases 1, 2, and 7.

$$D_{\bar{\nu}} = \sum_{i=1}^N \sum_{g=1}^G |S_{\bar{\nu},g}^{a,i} - S_{\bar{\nu},g}^{e,i}| ,$$

$$D_c = \sum_{i=1}^N \sum_{g=1}^G |S_{c,g}^{a,i} - S_{c,g}^{e,i}| ,$$

$$D_s = \sum_{i=1}^N \sum_{g=1}^G |S_{s,g}^{a,i} - S_{s,g}^{e,i}| ,$$

and

$$D_{sum} = D_{\bar{\nu}} + D_c + D_s , \quad (18)$$

where S is a simplified notation for the sensitivity coefficient as defined in Eq. (17) for the safety application a , or experimental configuration e , to the capture (c) or scattering (s) cross sections, or to $\bar{\nu}$ for energy group g and nuclide i with the total number of energy groups G and the total number of nuclides N .

The usefulness of these integral indices was demonstrated in that clear patterns could be detected when compared to traditional trending analyses for criticality safety validation.¹⁶ However, because these indices are unnormalized, the establishment of consistent limiting values was not possible. Therefore, an alternate form of sensitivity-based integral indices, denoted as E , was de-

veloped. These sensitivity-based indices correspond to the summation of the product of the sensitivity coefficients for two systems over energy groups and nuclides, normalized such that when summed over nuclides and reactions, an E value of 0.0 indicates the systems are totally dissimilar and an E value of 1.0 indicates the two systems are precisely the same. The E values are defined as

$$E_f = M^{-1} \sum_{i=1}^N \sum_{g=1}^G S_{f,g}^{a,i} S_{f,g}^{e,i} ,$$

$$E_c = M^{-1} \sum_{i=1}^N \sum_{g=1}^G S_{c,g}^{a,i} S_{c,g}^{e,i} ,$$

and

$$E_s = M^{-1} \sum_{i=1}^N \sum_{g=1}^G S_{s,g}^{a,i} S_{s,g}^{e,i} ,$$

where f , c , and s denote the fission, capture, and scattering reactions, respectively. The normalizing denominator is defined with a sum over x representing each reaction as

$$M = \sum_x \left\{ \sum_{i=1}^N \sum_{g=1}^G (S_{x,g}^{a,i})^2 \sum_{i=1}^N \sum_{g=1}^G (S_{x,g}^{e,i})^2 \right\}^{1/2} .$$

Finally, the summative value is defined as

$$E_{sum} = E_f + E_c + E_s . \quad (19)$$

If the groupwise sensitivity data for fission, capture, and scattering reactions for all nuclides for each system are thought of as vector, then the integral index E_{sum} is the cosine of the angle between the two sensitivity vectors for the analyzed systems. If the two sensitivity vectors are parallel, i.e., proportional, the systems are similar. Mathematically, an E_{sum} value as low as -1.0 could be generated, but this would be the result of a rare combination of system sensitivity coefficients such that the sensitivity of the respective system responses would have to be exactly proportional in magnitude and opposite in sign, which seems not to be physically feasible. As with the case of an E_{sum} value of 0.0 , this would indicate that the systems are dissimilar, or rather “antisimilar.” The E_{sum} parameter is considered global in nature because its single quantity assesses similarity between two systems based on the magnitude and shape of all sensitivity profiles for fission, capture, and scatter.

It is also possible and sometimes desirable to produce values analogous to E_{sum} for each isotope-reaction pair, such that similarity can be assessed on a reaction- and nuclide-specific level. For this purpose, an additional parameter dE is defined from the equations above by omitting the nuclide and reaction summations in the numerator and the reaction summation in the denominator. Thus, the dE value for reaction x of nuclide i between application a and experiment e is defined as

$$dE_{x,i}^{e,a} = \frac{\sum_{g=1}^G S_{x,g}^{a,i} S_{x,g}^{e,i}}{\left(\sum_{i=1}^N \sum_{g=1}^G (S_{x,g}^{a,i})^2 \sum_{i=1}^N \sum_{g=1}^G (S_{x,g}^{e,i})^2 \right)^{1/2}} . \quad (20)$$

The dE values relate, on a system-to-system basis, the similarity of various nuclide-reaction pairs. These values are normalized such that when an application is compared to itself, the sum over nuclides for a given reaction type (i.e., capture, fission, scatter) is 1.0 . This allows for similarity determinations for a particular reaction among various nuclides.

With the dE parameter, the particular nuclide-reaction pairs that cause two systems to be similar or dissimilar can be investigated. The magnitudes of the dE values show the relative contribution to E for each nuclide with respect to its capture, fission, or scattering reactions. In addition, since the normalization requires that the sum over a given reaction will be only 1.0 if the two systems are exactly the same, the sum over the dE values for each reaction gives an additional indicator of the systems’ similarity. A method of utilizing this information in a simple manner was to define a $T(E)$ value, which is the ratio of the dE value relating the two systems to the dE value of the application system related to itself. Thus,

the $T(E)$ value relating application a to experiment e for reaction x of nuclide i is

$$T(E)_{x,i}^{e,a} = \frac{dE_{x,i}^{e,a}}{dE_{x,i}^{a,a}} . \quad (21)$$

If the nuclide-reaction pair is less important in the benchmark experiment than the application, $T(E)$ has a value <1.0 . If the importance of the nuclide-reaction pair in the benchmark experiment is greater than or equal to the importance in the application, $T(E)$ is ≥ 1.0 . Thus, the number of benchmark systems with T values near or greater than 1.0 is an indicator of benchmark coverage for a given nuclide-reaction pair. Care must be taken in the use of $T(E)$ in that if the sensitivity for an experiment greatly exceeds that of the application for a portion of the spectrum, but is much less than the sensitivity of the application over another portion of the spectrum, an artificially high $T(E)$ value can result. Recent studies have investigated the development of a new parameter to address this difficulty.¹⁷

Returning to the example systems described in Sec. III.A, with sensitivity profiles shown in Fig. 2, the global E_{sum} values relating the first system to the second and the third are 0.9883 and 0.7223 , respectively. The $T(E)$ values for ^{235}U fission of the first system compared to the second and third are 0.9843 and 0.8484 , respectively. Since higher-valued integral indices represent more similarity, the methodology has quantified, on both a systemwide and nuclide-reaction specific basis, that the second system exhibits more similarities to the first than does the third.

IV. UNCERTAINTY ANALYSIS TECHNIQUES

An alternative and complementary approach to exploring the similarity of systems based solely on the use of sensitivity data is the use of uncertainty analysis, which propagates the tabulated cross-section uncertainty information to the calculated k_{eff} value of a given system via the sensitivity coefficients. This technique is similar to that employed in previous studies involving the validation of data for use in the design of fast reactors.¹⁸ Mathematically, the system uncertainty is computed with a quadratic product of the groupwise sensitivity profile vectors by nuclide and reaction type with the cross-section uncertainty matrices by nuclide and reaction type. The result of this procedure is not only an estimate of the uncertainty in the system k_{eff} due to cross sections but also an estimate of the correlated uncertainty between systems. These correlated uncertainties can be represented by correlation coefficients, which represent the degree of correlation in the uncertainties between the two systems. This parameter, denoted as c_k , not only has the desirability of a single quantity relating the two systems but also measures the similarity of the systems in

terms of related uncertainty, not just the related sensitivity. These correlation coefficients are particularly useful when used in traditional trending analyses for criticality safety validation in that the correlation coefficient relates the degree in which the uncertainties in the critical benchmarks are coupled with the uncertainties in the application of interest. This coupling with the common uncertainties in the various systems is expected to closely mimic the coupling in predicted biases between the various systems since they should both be related to the cross-section uncertainties. The underlying assumption in this approach is that the cross-section–uncertainty data for all nuclides and reactions of interest have been evaluated and processed for use by these procedures. However, evaluated cross-section–uncertainty data are not available for all nuclide–reaction pairs. Nuclide–reaction pairs without available data are omitted from this analysis, but it is assumed that either the cross-section data values from these pairs are well known (i.e., small uncertainties) or the sensitivity of the system k_{eff} to these nuclide–reaction pairs is small. Where these assumptions hold, the nuclide–reaction pairs without cross-section–uncertainty data present a negligible contribution to the uncertainty-based analysis. For situations where this negligible contribution assumption is judged not to be valid, the use of uncertainty analysis is not appropriate.

Two steps are required in the determination of the uncertainties in the calculated values of the system multiplication factor: (a) the estimation and processing of uncertainties in the cross-section data and (b) the propagation of those uncertainties to the systems k_{eff} values. The techniques for processing cross-section–uncertainty data are established^{19,20} and will not be discussed here. Cross-section–uncertainty data in the evaluated nuclear data files (i.e., ENDF/B-V) are limited to select isotopes; however, those data that are available have been processed for use with these techniques.

Given uncertainty information for the cross sections for all nuclides and reaction processes that are important to the system of interest, it is possible to estimate the uncertainty in the calculated system multiplication factor due to these data uncertainties.

The nuclear data parameters are represented by the vector $\alpha \equiv (\alpha_n)$, $n = 1, 2, \dots, M$, where M is the number of nuclide–reaction pairs \times the number of energy groups. The corresponding symmetric $M \times M$ matrix containing the relative variances (diagonal elements) and covariances (off-diagonal elements) in the nuclear data is

$$\mathbf{C}_{\alpha\alpha} \equiv \left[\frac{\text{cov}(\alpha_n, \alpha_p)}{\alpha_n \alpha_p} \right], \quad n = 1, 2, \dots, M; p = 1, 2, \dots, M, \quad (22)$$

where

$$\text{cov}(\alpha_n, \alpha_p) = \langle \delta\alpha_n \delta\alpha_p \rangle, \quad (23)$$

where $\delta\alpha_n$ and $\delta\alpha_p$ represent the difference between the values and expectation values of the nuclear data parameters and $\langle \rangle$ represents integration over the ranges of α_n and α_p weighted with a probability density function. A rigorous definition of the cross-section–covariance data is given in Ref. 21.

The matrix containing sensitivities of the calculated k_{eff} to the α parameters, where each matrix entry is consistent with Eq. (17), is given as

$$\mathbf{S}_k \equiv \left[\frac{\alpha_n}{k_i} \frac{\partial k_i}{\partial \alpha_n} \right], \quad i = 1, 2, \dots, I; n = 1, 2, \dots, M, \quad (24)$$

where I is the number of critical systems being considered. The uncertainty matrix for the system k_{eff} values, \mathbf{C}_{kk} , is given as

$$\mathbf{C}_{kk} = \mathbf{S}_k \mathbf{C}_{\alpha\alpha} \mathbf{S}_k^\dagger, \quad (25)$$

where \dagger indicates a transpose, \mathbf{S}_k is an $I \times M$ matrix, $\mathbf{C}_{\alpha\alpha}$ is an $M \times M$ matrix, and the resulting \mathbf{C}_{kk} matrix is of dimension $I \times I$. The \mathbf{C}_{kk} matrix consists of relative variance values σ_i^2 for each of the critical systems under consideration (the diagonal elements), as well as the relative covariance between systems σ_{ij}^2 (the off-diagonal elements). These off-diagonal elements represent the shared or common variance between two systems. The off-diagonal elements are typically divided by the square root of the corresponding diagonal elements (i.e., the respective standard deviations) to generate a correlation coefficient matrix. Thus, the correlation coefficient is defined as

$$c_k = \frac{\sigma_{ij}^2}{(\sigma_i \sigma_j)}, \quad (26)$$

such that the single c_k value represents the correlation coefficient between uncertainties in system i and system j .

These correlations are primarily due to the fact that the uncertainties in the calculated k_{eff} values for two different systems are related since they contain the same materials. Cross-section uncertainties propagate to all systems containing these materials. Systems with the same materials and similar spectra would be correlated, while systems with different materials or spectra would not be correlated. The interpretation of the correlation coefficient is the following: a value of 0.0 represents no correlation between the systems, a value of 1.0 represents full correlation between the systems, and a value of -1.0 represents a full anticorrelation.

Similar to the dE values defined previously, the nuclide–reaction specific components of c_k , denoted dc_k , are defined for comparison of specific nuclide–reaction pairs between a given application and experiment. A $T(c_k)$ parameter is defined as the ratio of the dc_k value for an experiment compared to an application to the dc_k value of the application compared to itself as

$$T(c_k)_{x_{eaj}} = \frac{dc_{k_{x_{eaj}}}}{dc_{k_{x_{aaj}}}}. \quad (27)$$

A $T(c_k)$ value of 1.0 or higher indicates that for a given nuclide reaction, the variance of the experiment is as great or greater than that of the application.

Again, returning to the example systems described in Sec. III.A, with sensitivity profiles shown in Fig. 2, the c_k values relating the first system to the second and the third are 0.9946 and 0.7520, respectively. The $T(c_k)$ values for ^{235}U fission for the first system and compared to the second and third are 1.0205 and 0.4588, respectively. Consistent with the conclusion reached in regard to these systems with the sensitivity-based integral indices, the uncertainty-based methodology has quantified, on both a systemwide and reaction-specific basis, that the second system exhibits more similarities to the first than does the third.

V. USE OF INTEGRAL INDICES AS TRENDING PARAMETERS

The integral indices E_{sum} and c_k can be used as trending parameters in criticality safety analysis validation studies. Using the same trending analysis tools described in Sec. II, but substituting either E_{sum} or c_k as the trending parameter, the computational bias and uncertainty can be determined. Because the integral indices measure the similarity of a benchmark experiment to an individual design system, a separate trending analysis must be conducted for each system of interest. This differs from the trending techniques presented in Sec. II, where the bias, uncertainty, and USL are determined as a function of the specified trending parameter, and then the bias and uncertainty functions are evaluated at the value of the trending parameter corresponding to each design system that falls within the range of applicability of that parameter. Because of the definitions and normalizations of the integral indices E_{sum} and c_k when used as trending parameters, the evaluation of the bias and uncertainty will always occur at the trending parameter value of 1.0, which corresponds to the design system. Furthermore, all benchmark experiments will have an E_{sum} or c_k value < 1.0 in relation to a design system. Thus, the evaluation of the bias and uncertainty will always require some degree of extrapolation outside the range of the trending parameters, as shown in the right side of Fig. 1. The evaluation of the computation bias is achieved through the same linear regression of the k_{eff} values as is used in the calculation of USL_1 and USL_2 , but the uncertainty in the bias should be evaluated using $w(t)$, the functional confidence band, instead of W , the maximum value of $w(t)$ within the range of the trending parameters. Some sample trending analyses, comparing the use of various trending parameters, are presented in Sec. VII.

VI. GENERALIZED LINEAR-LEAST-SQUARES TECHNIQUES

The GLLSM provides an alternative approach to traditional trending analysis for the determination of computational biases. The GLLSM predicts cross-section data adjustments that would produce the best agreement between the measured and calculated values of k_{eff} based on the entire set of benchmark experiments used in the data validation process.²² The effect of these cross-section adjustments is then estimated through propagation to the computed k_{eff} , via the sensitivity coefficients, for any system determined to be within the area of applicability of the chosen benchmark experiments. The difference between the k_{eff} values computed with the standard cross-section data and those computed with the adjusted cross-section data gives an assessment of the computational bias. The inputs needed for such an analysis are almost identical to those used in the S/U methods presented thus far: the sensitivity coefficients, the cross-section uncertainties, and the calculated k_{eff} values. Additionally, estimates of the uncertainties in the measured k_{eff} values of the benchmark experiments are also required.

One of the benefits of the GLLSM approach is that not only can the bias for a given application be estimated based on a particular set of benchmarks, but also the effect on the bias of the inclusion or exclusion of benchmark experiments can be determined. The adequacy of the benchmark set chosen for validation can be verified with this procedure. GLLSM can address how many experiments are needed and how much correlation is necessary to validate criticality codes within a particular area of applicability.

VI.A. GLLSM Theory

The GLLSM has been referred to as a data adjustment procedure, a data consistency analysis, and even a data evaluation technique. The most appropriate description of GLLSM for this particular application is that of a generalized trending analysis tool. The GLLSM “forces” agreement between the measured and calculated values of k_{eff} for the entire set of benchmark experiments used in the data validation process. The data adjustments that result from the application of the GLLSM can then be used to predict the biases for any application determined to be within the area of applicability of the benchmark experiments used in the GLLSM analysis. Functionally, the GLLSM can be thought of as a trending of a suite of critical benchmarks with respect to the cross-section correlation coefficient between the various systems. The GLLSM has the capability of identifying experiments that contain inconsistencies (i.e., the magnitude of the measured-to-calculated k_{eff} difference is larger than their combined uncertainties). A χ^2 -consistency indicator is used to directly predict the overall consistency of the

suite of benchmarks. A value of χ^2 for each experiment is also available from the GLLSM tool.

The vector $\mathbf{m} \equiv (m_i)$, $i = 1, 2, \dots, I$, represents a series of k_{eff} measurements on I critical benchmark experiments that are to be used in the validation of a code and dataset over a particular area of applicability for criticality safety computations. The elements of the $I \times I$ matrix of the relative uncertainties in the measurements are given by

$$\left[\frac{\text{cov}(m_i, m_j)}{m_i m_j} \right], \quad i = 1, \dots, I, j = 1, \dots, I \quad (28)$$

For consistency with adjustments relative to the calculated k_{eff} values, the elements of relative uncertainty matrix for the measured values \mathbf{C}_{mm} are defined as²³

$$\left(\frac{m_i}{k_i} \right) \left[\frac{\text{cov}(m_i, m_j)}{m_i m_j} \right] \left(\frac{m_j}{k_j} \right), \quad i = 1, \dots, I; j = 1, \dots, I, \quad (29)$$

where the elements of the vector $\mathbf{k} \equiv (k_i)$, $i = 1, 2, \dots, I$, are the corresponding calculated values of k_{eff} for each of these experiments. The GLLSM procedure also allows for the possibility of correlations between the integral and differential quantities. The elements of this $M \times I$ relative cross-covariance are

$$\left[\frac{\text{cov}(\alpha_n, m_i)}{\alpha_n m_i} \right], \quad n = 1, 2, \dots, M; i = 1, 2, \dots, I \quad (30)$$

Similar to the definition in Eq. (29), the elements of the relative uncertainty matrix for the cross-correlations \mathbf{C}_{am} are defined relative to the calculated k_{eff} as

$$\left[\frac{\text{cov}(\alpha_n, m_i)}{\alpha_n m_i} \right] \left(\frac{m_i}{k_i} \right), \quad n = 1, \dots, M; i = 1, \dots, I \quad (31)$$

The correlations given in Eq. (31) are not yet included in this implementation of GLLSM but are carried through this theoretical derivation.

Linear changes in the calculated k_{eff} values due to perturbations in α can be represented as

$$\begin{aligned} k_i(\alpha') &= k_i(\alpha + \delta\alpha) = k_i(\alpha) + \delta k_i \\ &\equiv k_i(\alpha) \left[1 + \sum_{n=1}^M S_n^i \frac{\delta\alpha_n}{\alpha_n} \right], \end{aligned} \quad (32)$$

where α' is an adjusted set of nuclear data parameters defined as the original parameters with some perturbation $\delta\alpha$; $\mathbf{k}(\alpha)$ and $\mathbf{k}(\alpha')$ represent the calculated k_{eff} values using the standard and adjusted data sets, respectively. The sensitivity coefficient S_n^i represents the relative sensitivity of the k_{eff} of system i to perturbations in nuclear parameter α_n .

The relative deviations of the calculated responses from their corresponding measured values are denoted with the vector \mathbf{d} , the elements of which are

$$(d_i) = \frac{k_i(\alpha) - m_i}{k_i(\alpha)}, \quad i = 1, \dots, I \quad (33)$$

The uncertainty matrix for the absolute deviation vector taken relative to the calculational k_{eff} values is

$$\begin{aligned} \mathbf{C}_{dd} &= \mathbf{C}_{kk} + \mathbf{C}_{mm} - \mathbf{S}_k \mathbf{C}_{am} - \mathbf{C}_{ma} \mathbf{S}_k^\dagger, \\ &= \mathbf{S}_k \mathbf{C}_{aa} \mathbf{S}_k^\dagger + \mathbf{C}_{mm} - \mathbf{S}_k \mathbf{C}_{am} - \mathbf{C}_{ma} \mathbf{S}_k^\dagger. \end{aligned} \quad (34)$$

The elements of the M -dimensional vector \mathbf{z} are the relative changes in parameters α_n such that

$$z_n = \frac{\alpha'_n - \alpha_n}{\alpha_n} = \frac{\delta\alpha_n}{\alpha_n}.$$

The elements of the vector \mathbf{y} are the resulting deviations of the calculated k_{eff} values from their respective measured values m_i relative to the original calculated values $k_i(\alpha)$ such that

$$y_i = \frac{m'_i - m_i}{k_i} = \frac{k_i(\alpha') - m_i}{k_i(\alpha)}.$$

The vector $\mathbf{m}' \equiv (m'_i)$, $i = 1, \dots, I$ represents the best estimates of the k_{eff} values. Using these definitions, Eq. (32) can be rewritten as

$$\mathbf{y} = \mathbf{d} + \mathbf{S}_k \mathbf{z} \quad (35)$$

The measured k_{eff} values \mathbf{m} and the measured (or evaluated from measurements) parameter values α both have their corresponding uncertainties. The best evaluated parameters α' and the best evaluated k_{eff} values \mathbf{m}' will be those values that are consistent with each other, namely, $\mathbf{m}' = \mathbf{k}(\alpha')$. Additionally, \mathbf{m}' and α' are consistent with their estimated values and uncertainties in that they do not deviate from the stated values of \mathbf{m} and α by more than the respectively stated uncertainties.

The GLLSM procedure involves minimizing the quadratic loss function

$$Q(\mathbf{z}, \mathbf{y}) = (\mathbf{y}, \mathbf{z})^\dagger \begin{pmatrix} \mathbf{C}_{mm} & \mathbf{C}_{m\alpha} \\ \mathbf{C}_{am} & \mathbf{C}_{aa} \end{pmatrix}^{-1} (\mathbf{y}, \mathbf{z}), \quad (36)$$

where $(\mathbf{y}, \mathbf{z})^\dagger \equiv (y_1, y_2, \dots, y_I, z_1, z_2, \dots, z_M)$, subject to the constraint expressed by Eq. (35). Adopting the procedure of Ref. 16, the foregoing conditional minimum formulation is equivalent to unconditionally minimizing the function $R(\mathbf{z}, \mathbf{y})$, where

$$R(\mathbf{z}, \mathbf{y}) = Q(\mathbf{z}, \mathbf{y}) + 2\lambda^\dagger (\mathbf{S}_k \mathbf{z} - \mathbf{y}) \quad (37)$$

and $\boldsymbol{\lambda}$ is an i -dimensional vector of Lagrange multipliers. Thus \mathbf{z} and \mathbf{y} satisfy the equation

$$\frac{\partial R(\mathbf{z}, \mathbf{y})}{\partial \mathbf{z}} = \frac{\partial R(\mathbf{z}, \mathbf{y})}{\partial \mathbf{y}} = 0 . \quad (38)$$

Solving the resulting equations for \mathbf{z} and \mathbf{y} , one obtains

$$\mathbf{z} = (\mathbf{C}_{am} - \mathbf{C}_{\alpha\alpha} \mathbf{S}_k^\dagger) \mathbf{C}_{dd}^{-1} \mathbf{d}$$

and

$$\mathbf{y} = (\mathbf{C}_{mm} - \mathbf{C}_{m\alpha} \mathbf{S}_k^\dagger) \mathbf{C}_{dd}^{-1} \mathbf{d} , \quad (39)$$

where the $I \times I$ matrix \mathbf{C}_{dd}^{-1} is the inverse of \mathbf{C}_{dd} in Eq. (34).

A few observations are due here:

1. If the $\boldsymbol{\alpha}'$ values obtained in Eq. (39) are substituted in $\mathbf{k}(\boldsymbol{\alpha})$, using the linearity assumption of Eq. (32), then $\mathbf{m}' = \mathbf{k}(\boldsymbol{\alpha}')$ is satisfied.
2. Moreover, not only are the new/best estimates of the cross sections and of the k_{eff} values consistent, but their uncertainties are reduced as well.

These reduced relative uncertainties are given by

$$\mathbf{C}_{m'm'} = \mathbf{C}_{mm} - \mathbf{C}_{yy}$$

and

$$\mathbf{C}_{\alpha'\alpha'} = \mathbf{C}_{\alpha\alpha} - \mathbf{C}_{zz} , \quad (40)$$

where

$$\mathbf{C}_{yy} = (\mathbf{C}_{mm} - \mathbf{C}_{m\alpha} \mathbf{S}_k^\dagger) \mathbf{C}_{dd}^{-1} (\mathbf{C}_{mm} - \mathbf{S}_k \mathbf{C}_{am})$$

and

$$\mathbf{C}_{zz} = (\mathbf{C}_{am} - \mathbf{C}_{\alpha\alpha} \mathbf{S}_k^\dagger) \mathbf{C}_{dd}^{-1} (\mathbf{C}_{m\alpha} - \mathbf{S}_k \mathbf{C}_{\alpha\alpha}) . \quad (41)$$

This suggests that any criticality application that is similar to the selected benchmarks should be calculated using the modified cross sections and thus have a reduced uncertainty. However, even when maintaining conventional criticality estimates using established cross sections and trend curves, the GLLSM approach can be beneficial, as will be demonstrated in Sec. VI.B.

In summary, the GLLSM procedure as applied to the validation of cross-section libraries and codes for criticality safety applications is designed to predict the data relative changes \mathbf{z} such that the differences between measured and calculated k_{eff} values (i.e., \mathbf{y}) are minimized. These k_{eff} differences are the trends observed in the traditional criticality safety trending analyses. Removal of these trends and the identification of the data responsible for them are keys to the application of GLLSM techniques to criticality safety data validation.

VI.B. Application of GLLSM to Data Validation

The solution of Eq. (39) allows evaluation of the \mathbf{z} and \mathbf{y} quantities in Eq. (35). Of particular interest is the quantity \mathbf{d} , whose elements are defined in Eq. (33). This quantity is the relative calculated-versus-measured discrepancy in k_{eff} as determined from the as-specified experimental benchmark description and given cross sections. For a criticality safety application for which the computational bias must be assessed, the single measured value m_a associated with the calculated value of k_{eff} , $k_a(\boldsymbol{\alpha})$, does not exist. Rewriting Eq. (35) for the application and substituting the value of m'_a for m_a , thus using the best estimate of the measured values, we obtain

$$\frac{k_a(\boldsymbol{\alpha}') - m'_a}{k_a(\boldsymbol{\alpha})} = \frac{k_a(\boldsymbol{\alpha}) - m'_a}{k_a(\boldsymbol{\alpha})} + \mathbf{S}_a \mathbf{z} , \quad (42)$$

where \mathbf{S}_a is an M -dimensional row vector of the calculated sensitivities for the design application. The GLLSM theory predicts that if a sufficient number of experiments are similar to the application of interest, the calculated value of k_{eff} , using the best adjusted cross sections $\boldsymbol{\alpha}'$, will indeed approach the value m'_a ; thus, $k_a(\boldsymbol{\alpha}') - m'_a = 0$, and Eq. (42) yields the predicted value of the application bias

$$\beta_a = k_a(\boldsymbol{\alpha}) - m'_a , \quad (43)$$

which is also obtained when using the standard and adjusted cross section as

$$\beta_a \cong -k_a(\boldsymbol{\alpha}) \cdot \mathbf{S}_a \mathbf{z} , \quad (44)$$

where \mathbf{z} is obtained in Eq. (39) using all similar benchmark criticality measurements.

The uncertainty in the adjusted value of k_{eff} , $k_a(\boldsymbol{\alpha}')$, is obtained by propagating the adjusted cross-section-covariance matrix $\mathbf{C}_{\alpha'\alpha'}$ defined in Eq. (40) to the uncertainty in k_{eff} as

$$\mathbf{C}_{k'k'} = \mathbf{S}_k \mathbf{C}_{\alpha'\alpha'} \mathbf{S}_k^\dagger . \quad (45)$$

The definitions of a similar and sufficient number of experiments necessary for accurate convergence of the methodology are determined by tests using actual benchmark experiments and are discussed in Sec. VIII.

VII. TRENDING ANALYSIS EXAMPLES

Some illustrative applications of the techniques outlined in this paper are given below. The sensitivity data for each of the systems included in this analysis were generated using the TSUNAMI-1D (formerly SEN1) (Ref. 5) or TSUNAMI-3D (formerly SEN3) (Ref. 6) sensitivity analysis sequence within a prerelease of version 5 of SCALE (Ref. 4), SCALE 5. The k_{eff} value for

each system was also generated with the criticality calculation of the sensitivity analysis. The integral parameters c_k , E_{sum} , $T(c_k)$, and $T(E)$ were generated using the TSUNAMI-IP (formerly CANDE) code within the prerelease version of SCALE 5. The cross-section-covariance data were obtained from the PUFF-II code.²⁴ In all cases, the criticality and sensitivity calculations were performed with the 44-energy-group neutron-cross-section data library of SCALE, which is based on ENDF/B-V data.

These example calculations correspond to the validation of criticality safety studies for facilities processing uranium fuels with enrichments >5 wt% in ^{235}U for use in commercial power reactors. Currently, uranium processing facilities are limited to enrichments at or below 5 wt%, and much of the available benchmark experiment data correspond to these lower enrichments.

The goal of these exercises is to estimate the bias trends for ranges over which the criticality safety computational studies are to be performed. For this example, a hypothetical set of four systems that could be encountered in the design of a uranium processing facility was conceived. Each design system consists of critical bare spheres of UO_2 fuel enriched to 11 wt% in ^{235}U with H/X values varying from 0 to 500. The 11 wt% enrichment was chosen so the entire range of moderation conditions, including dry, could be studied in a critical configuration. The H/X values, critical radii, and computed EALF values for these four sample design systems are presented in Table I. Data validations for these systems were performed using traditional trending analyses, trending analyses with the S/U integral indices E_{sum} and c_k , and the GLLSM approach. Advantages and disadvantages of each approach are explored, and guidance for the general use of these techniques is developed.

VII.A. Description of Benchmark Systems

A suite of 100 available benchmark experiments was prepared for this study. These experiments were selected

TABLE I

Specifications for Example Applications
Consisting of Bare $\text{U}(11)\text{O}_2$ Spheres

H/X	Critical Radius (cm)	EALF (eV)	Uncertainty in Calculated k_{eff} due to Cross-Section Data Uncertainties (% standard deviation)
0	50.55	165 700	1.8659
3	40.00	7 813	1.8634
40	22.34	2.269	1.3566
500	21.42	0.04571	0.9328

to represent a wide range of uranium-fueled systems such that the capabilities of S/U methods could be demonstrated. This experiment suite, which is further documented in Ref. 16, is summarized in Table II of this paper. The first 12 experiments in Table II are low-enrichment uranium oxide or fluoride systems with 2 to 5 wt% uranium fuel and paraffin or stereotex moderators. Fifteen experiments (13 through 17; 28 through 32; 44, 45, and 46; and 49 and 50 in Table II) were developed by the Cross-Section Evaluation Working Group as data-testing benchmarks and cover a full range of enrichments from ~ 1 to 93 wt%, dry to fully moderated. Eleven experiments (33 through 43) are Physical Constants Testing Reactor (PCTR) infinite multiplication factor k_∞ experiments on 2 wt% enriched uranium fuel. Eight experiments (20 through 27) are high-enrichment uranium (HEU) metal experiments (HEUMET), and eight experiments (57 through 64) are low-H/X Rocky Flats experiments (RF) with uranium enrichments of 4.5 wt%. Thirty-six experiments (65 through 100), obtained from the IHECSBE, were performed in Russia with various configurations of solution tanks and fuel rod arrays with ^{235}U enrichments ranging from 5 to 89 wt%. An additional ten various experiments (18 and 19, 47 and 48, and 51 through 56) include HISS, UH_3 , and LXX configurations described in Ref. 16.

For this demonstration analysis, the SEN1 code was used to calculate the criticality and sensitivity data of systems for which reliable one-dimensional (1-D) models were available. TSUNAMI-3D was used to calculate the data for more complex systems, which required Monte Carlo analysis. One exception is the ICT series of hexagonally pitched arrays. In this case, the CSAS26 analysis sequence of SCALE using the KENO-VI Monte Carlo code was used to generate the criticality data based on a three-dimensional model, and the SEN1 sequence was used to generate the sensitivity data based on a 1-D system model.

VII.B. Traditional Trending Analysis

In order to clearly show the relationship between the S/U techniques and the traditional techniques for criticality safety validations, a traditional trending analysis of the four $\text{U}(11)\text{O}_2$ design systems was performed based on the 100 benchmark experiments. For this analysis the USLSTATS computer program² was applied to compute the USL_1 and USL_2 , defined in Eqs. (3) and (4), in order to determine the limiting values of k_{eff} as a function of EALF and H/X for the selected suite of benchmark experiments. The trending of k_{eff} as a function of EALF is shown in Fig. 3, and the trending of k_{eff} as a function of H/X is shown in Fig. 4. The area of applicability of the chosen experiments includes EALF values from 0.0295 to 904 000 eV and H/X ratios from 0 to 1840, as shown in Table II. Since the $\text{U}(11)\text{O}_2$ design systems have EALF values of 0.04571 to 165 700 eV and H/X ratios of 0 to

TABLE II
Specifications of 100 Benchmark Experiments Selected for Example Validation Study

System Number	Identifier	Code ^a	Calculated $k_{eff} \pm \sigma$ (standard deviation of Monte Carlo)	Uncertainty in Calculated k_{eff} due to Cross-Section Data Uncertainties (% standard deviation)	Measured k_{eff} Value	Reported Uncertainty in Measured k_{eff} (% standard deviation)	(Measured/Calculated) - 1 (%)	EALF	H/X
1	U(2)F4 - 195	1	1.0022	1.16	1.0000	0.5	-0.65	2.37E-01 ^b	195
2	U(2)F4 - 294	1	1.0038	1.05	1.0000	0.4	-0.79	1.32E-01	294
3	U(2)F4 - 406	1	1.0010	0.98	1.0000	0.5	-0.49	9.15E-02	406
4	U(2)F4 - 496	1	0.9991	0.95	1.0000	0.4	-0.29	7.57E-02	496
5	U(2)F4 - 614	1	0.9984	0.91	1.0000	0.4	-0.20	6.36E-02	614
6	U(2)F4 - 972	1	0.9926	0.86	1.0000	0.5	0.46	4.75E-02	972
7	U(5)3O8 - 147	1	0.9973	1.07	1.0000	0.4	0.36	2.05E-01	147
8	U(5)3O8 - 245	1	0.9844	0.99	1.0000	0.4	1.63	1.00E-01	245
9	U(5)3O8 - 320	1	1.0079	0.95	1.0000	0.4	-0.76	7.49E-02	320
10	U(5)3O8 - 396	1	1.0021	0.92	1.0000	0.3	-0.21	6.26E-02	396
11	U(5)3O8 - 503	1	1.0012	0.90	1.0000	0.3	-0.13	5.26E-02	503
12	U(5)3O8 - 757	1	1.0035	0.86	1.0000	0.3	-0.38	4.21E-02	757
13	Godiva	1	1.0014	1.61	1.0000	0.1	-0.41	9.04E+05	0
14	Bapl-1	1	1.0003	0.96	1.0000	NR	-0.17	2.03E-01	306
15	Bapl-2	1	0.9999	0.91	1.0000	NR	-0.16	1.53E-01	382
16	Bapl-3	1	0.9998	0.85	1.0000	NR	-0.23	1.13E-01	515
17	Big-10	1	1.0168	2.05	1.0000	0.3	-1.70	4.80E+05	0
18	HISS (HUG)	1	1.0120	2.07	1.0000	0.4	-1.18	1.47E+02	0
19	U(98) H2O refl.	1	0.9999	1.38	1.0000	0.5	0.14	2.80E+04	0
20	HEUMET A	1	0.9899	1.62	1.0000	0.5	1.21	8.79E+05	0
21	HEUMET B	1	0.9877	1.61	1.0000	0.5	1.37	8.75E+05	0
22	HEUMET C	1	0.9917	1.59	1.0000	0.5	0.90	8.68E+05	0
23	HEUMET D	1	0.9899	1.57	1.0000	0.3	1.04	8.62E+05	0
24	HEUMET E	1	0.9955	1.59	1.0000	0.3	0.45	8.45E+05	0
25	HEUMET F	1	0.9965	1.58	1.0000	0.3	0.34	8.36E+05	0
26	HEUMET G	1	0.9987	1.57	1.0000	0.3	0.12	8.13E+05	0
27	HEUMET H	1	1.0227	2.36	1.0000	0.5	-0.48	7.08E+05	0
28	ORNL-1	1	0.9984	0.83	1.0000	0.3	0.10	3.09E-02	1378
29	ORNL-2	1	0.9982	0.82	1.0000	0.3	0.13	3.23E-02	1177
30	ORNL-3	1	0.9952	0.81	1.0000	0.3	0.43	3.37E-02	1033
31	ORNL-4	1	0.9966	0.81	1.0000	0.3	0.29	3.44E-02	972
32	ORNL-10	1	0.9986	0.80	1.0000	0.3	0.09	2.95E-02	1835
33	PCTR 3.73	1	1.0332	1.16	1.0310	0.6	-0.31	2.30E-01	322
34	PCTR 3.78	1	1.0089	1.17	1.0050	0.6	-0.49	2.24E-01	353
35	PCTR 3.83	1	0.9887	1.16	0.9860	0.6	-0.37	2.20E-01	381
36	PCTR 5.84	1	1.0088	1.03	1.0050	0.6	-0.47	1.23E-01	545
37	PCTR 5.99	1	1.0361	1.03	1.0310	0.6	-0.58	1.19E-01	518
38	PCTR 6.23	1	0.9820	1.02	0.9860	0.6	0.32	1.15E-01	619
39	PCTR 6.9	1	1.0284	1.00	1.0300	0.6	0.07	1.02E-01	619
40	PCTR 6.95	1	0.9742	1.00	0.9740	0.6	-0.10	1.02E-01	596
41	PCTR 7.14	1	0.9962	0.99	0.9920	0.6	-0.51	9.86E-02	667
42	PCTR 7.52	1	0.9670	0.98	0.9600	0.6	-0.80	9.43E-02	748
43	PCTR 7.52a	1	1.0217	0.98	1.0190	0.6	-0.34	9.33E-02	650
44	ZPR 3/11	1	1.0188	1.90	1.0000	0.3	-1.97	4.53E+05	0
45	ZPR 3/12	1	1.0123	1.56	1.0000	0.2	-1.36	3.01E+05	0
46	ZPR 6/6a	1	1.0224	1.79	1.0000	0.1	-2.41	6.86E+04	0
47	UH3 NI	1	1.0201	2.29	1.0000	NR	-1.07	2.35E+03	0
48	UH3 UR	1	1.0030	1.56	1.0000	NR	-0.71	1.09E+04	0
49	TRX-1	1	0.9928	0.93	1.0000	NR	0.53	3.25E-01	251
50	TRX-2	1	0.9960	0.82	1.0000	NR	0.25	1.65E-01	429
51	ORNL L7	1	1.0058	1.11	1.0000	NR	-0.53	1.58E-01	76
52	ORNL L8	1	1.0058	0.85	1.0004	NR	-0.63	3.21E-02	1110
53	ORNL L9	1	1.0029	0.83	1.0000	NR	-0.34	3.08E-02	1390
54	ORNL L10	1	1.0033	1.04	1.0000	NR	-0.29	8.90E-02	126

(Continued)

TABLE II (Continued)

System Number	Identifier	Code ^a	Calculated $k_{eff} \pm \sigma$ (standard deviation of Monte Carlo)	Uncertainty in Calculated k_{eff} due to Cross-Section Data Uncertainties (% standard deviation)	Measured k_{eff} Value	Reported Uncertainty in Measured k_{eff} (% standard deviation)	(Measured/Calculated) - 1 (%)	EALF	H/X
55	ORNL L11	1	1.0011	0.83	0.9999	NR	-0.16	3.09E-02	1270
56	SHEBA	3	1.0025 ± 0.0004	0.92	1.0000	NR	-0.88	6.17E-02	405
57	RF 0.77 A	3	0.9986 ± 0.0007	1.33	1.0000	0.1	-0.37	4.93E+02	17
58	RF 0.77 B	3	1.0075 ± 0.0007	1.05	1.0000	0.1	-1.15	4.04E+00	17
59	RF 0.77 C	3	1.0035 ± 0.0006	0.86	1.0000	0.1	-0.61	2.14E+00	17
60	RF 0.77 D	3	1.0125 ± 0.0006	1.08	1.0000	0.1	-1.06	5.72E+00	17
61	RF 2.03 A	3	1.0065 ± 0.0004	1.03	1.0000	0.1	-0.62	6.98E-01	70.7
62	RF 2.03 B	3	1.0086 ± 0.0004	0.88	1.0000	0.1	-1.04	3.20E-01	120.1
63	RF 2.03 C	3	1.0052 ± 0.0006	1.16	1.0000	0.1	-0.65	4.02E+00	45
64	RF 2.03 D	3	0.9986 ± 0.0005	1.18	1.0000	0.1	-0.01	3.68E+00	45
65	HST29-1	3	1.0054 ± 0.0005	1.02	1.0000	0.7	-0.32	1.54E-01	92
66	HST29-2	3	1.0079 ± 0.0005	0.99	1.0000	0.6	-0.62	1.53E-01	92
67	HST29-3	3	1.0019 ± 0.0005	0.98	1.0000	0.7	-0.02	1.55E-01	92
68	HST29-4	3	0.9991 ± 0.0004	0.96	1.0000	0.7	0.36	1.62E-01	92
69	HST29-5	3	1.0034 ± 0.0004	0.97	1.0000	0.7	-0.15	1.65E-01	92
70	HST29-6	3	1.0050 ± 0.0005	0.99	1.0000	0.7	-0.50	1.65E-01	92
71	HST29-7	3	1.0049 ± 0.0005	1.01	1.0000	0.6	-0.31	1.64E-01	92
72	HST30-1	3	1.0003 ± 0.0005	0.93	1.0000	0.4	-0.02	4.54E-02	375
73	HST30-2	3	1.0010 ± 0.0005	0.88	1.0000	0.3	-0.06	4.61E-02	375
74	HST30-3	3	0.9991 ± 0.0004	0.86	1.0000	0.3	0.05	4.64E-02	375
75	HST30-4	3	1.0063 ± 0.0005	1.19	1.0000	0.6	-0.46	1.54E-01	92
76	HST30-5	3	1.0031 ± 0.0005	1.02	1.0000	0.6	-0.06	1.56E-01	92
77	HST30-6	3	1.0048 ± 0.0005	1.00	1.0000	0.6	-0.24	1.56E-01	92
78	HST30-7	3	1.0038 ± 0.0004	0.97	1.0000	0.6	-0.07	1.61E-01	92
79	HST31-1	3	1.0036 ± 0.0005	0.99	1.0000	0.5	-0.12	1.59E-01	92
80	HST31-2	3	1.0051 ± 0.0005	0.94	1.0000	0.6	-0.35	1.70E-01	92
81	HST31-3	3	1.0029 ± 0.0005	0.98	1.0000	0.6	-0.27	1.64E-01	92
82	HST31-4	3	1.0015 ± 0.0004	0.96	1.0000	0.7	0.00	1.84E-01	92
83	ICT02-1	6	0.9944 ± 0.0011	0.84	1.0000	0.4	0.56	8.17E-02	628
84	ICT02-2	6	0.9927 ± 0.0012	0.88	1.0000	0.4	0.74	1.23E-01	628
85	ICT02-3	6	0.9997 ± 0.0012	0.81	1.0000	0.4	0.03	9.34E-02	611
86	ICT02-4	6	0.9953 ± 0.0012	0.82	1.0000	0.4	0.47	1.24E-01	611
87	ICT02-5	6	0.9927 ± 0.0013	0.81	1.0000	0.4	0.74	9.31E-02	562
88	ICT02-6	6	0.9915 ± 0.0012	0.82	1.0000	0.4	0.86	1.23E-01	562
89	LCT32-1	3	1.0029 ± 0.0004	1.04	1.0000	0.4	0.23	7.00E-01	50
90	LCT32-2	3	1.0033 ± 0.0004	1.16	1.0000	0.4	0.89	9.28E-01	50
91	LCT32-3	3	1.0032 ± 0.0004	1.16	1.0000	0.4	1.20	1.34E+00	50
92	LCT32-4	3	1.0082 ± 0.0004	0.85	1.0000	0.4	-0.94	6.85E-02	340
93	LCT32-5	3	1.0027 ± 0.0004	0.86	1.0000	0.3	0.23	1.03E-01	340
94	LCT32-6	3	1.0037 ± 0.0004	0.87	1.0000	0.3	0.18	1.21E-01	340
95	LCT32-7	3	1.0096 ± 0.0003	0.81	1.0000	0.5	-0.78	5.35E-02	629
96	LCT32-8	3	1.0105 ± 0.0004	0.82	1.0000	0.4	-0.20	7.83E-02	629
97	LCT32-9	3	1.0101 ± 0.0004	0.83	1.0000	0.4	-0.26	9.08E-02	629
98	LST05-1	3	0.9980 ± 0.0003	0.90	1.0000	0.4	0.12	3.87E-02	973
99	LST05-2	3	0.9984 ± 0.0003	0.90	1.0000	0.5	0.11	3.88E-02	973
100	LST05-3	3	0.9982 ± 0.0003	0.89	1.0000	0.6	0.11	3.90E-02	973

^a1: TSUNAMI-1D used to calculate all data, 3: TSUNAMI-3D used to calculate all data, 6: CSAS26 used to calculate k_{eff} data, and TSUNAMI-1D used to calculate sensitivity data.

^bRead as 2.37×10^{-1} .

500, complete coverage for the use of traditional trending techniques is demonstrated. The predicted bias; uncertainty in the bias, W in Eq. (3); and the USL_1 values for the four design systems are given in Table III. The

predictions from this analysis are a positive bias of 0.15 to 0.37%. The limiting USL_1 value, which treats a positive bias as a bias of zero, is 0.9370, based on the H/X trending results.

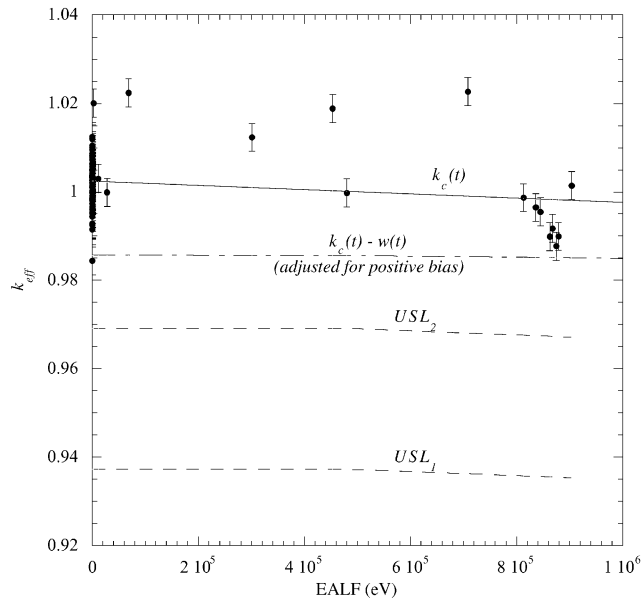


Fig. 3. Trend plot of k_{eff} versus EALF for 100 benchmark experiments.

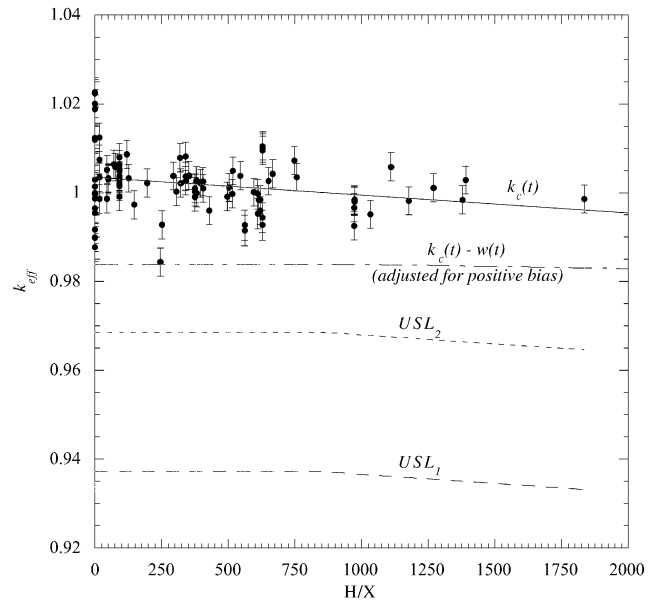


Fig. 4. Trend plot of k_{eff} versus H/X for 100 benchmark experiments.

VII.C. Trending Analysis with Integral Parameter Techniques

In this section, trending analyses using the same set of 100 benchmarks as was used in the traditional analyses are performed using the E_{sum} and c_k coefficients as the trending parameters. Even though it is possible to perform the trending on each of the E coefficients independently, it was decided to trend k_{eff} versus the sum of these coefficients (i.e., $E_{sum} = E_c + E_f + E_s$). This combination reduces the number of trend plots to be examined and provides a comprehensive measure of system similarity. Consistent with traditional trending analysis, the S/U trending analyses presented in this section were performed with the USLSTATS computer program. In place of the traditional trending parameters, the values

of E_{sum} and c_k for the specific application analyzed were input to the program. The bias and its uncertainty were assessed at an E_{sum} or c_k value of 1.0, which by definition of these indices corresponds to the design system. The trending methodology described in Sec. V was followed with the administrative margin set at 5%.

Prior to the trending analysis, a full set of sensitivity coefficients, detailing the groupwise sensitivity of k_{eff} to each nuclide-reaction pair, was generated for each of the design systems and for each of the 100 experimental benchmarks. These data were then utilized in the TSUNAMI-IP code to generate the integral parameters E_{sum} and c_k , demonstrating the similarity of each benchmark experiment to each design system. The standard deviations in the calculated values of k_{eff} due to evaluated uncertainties in the cross-section data were

TABLE III

Comparison of Predicted U(11)O₂ Δk Bias, Uncertainty in the Bias, and USL₁ for Various Procedures

Procedure	H/X = 0			H/X = 3			H/X = 40			H/X = 500		
	β (%)	$\Delta\beta$ (%)	USL ₁	β (%)	$\Delta\beta$ (%)	USL ₁	β (%)	$\Delta\beta$ (%)	USL ₁	β (%)	$\Delta\beta$ (%)	USL ₁
EALF	0.18	1.30	0.9370	0.24	1.30	0.9370	0.24	1.30	0.9370	0.24	1.30	0.9370
H/X	0.37	1.30	0.9370	0.37	1.30	0.9370	0.35	1.30	0.9370	0.15	1.30	0.9370
E_{sum}	0.70	1.29	0.9371	1.16	1.27	0.9359	0.22	1.26	0.9374	0.13	1.24	0.9376
c_k	0.76	1.29	0.9371	0.90	1.27	0.9360	0.17	1.30	0.9373	0.16	1.24	0.9376
GLLSM	2.49	0.31		1.39	0.25		0.74	0.13		0.21	0.11	

also computed and are presented in Table I for the U(11)O₂ systems and in Table II for the experimental benchmarks. The uncertainties for the U(11)O₂ systems range from 0.85 to 1.87%, and the uncertainties for the benchmark experiments range from 0.80 to 2.36%. The highest uncertainties correspond to the lowest H/X values because a harder neutron spectrum enhances the sensitivity to the higher-energy cross sections, which typically have higher uncertainties than the thermal values.

Where the ranges of the EALF and H/X values for the benchmark experiments were used to demonstrate that the U(11)O₂ design systems fell within the area of applicability of the suite of experiments for traditional validation techniques, the E_{sum} and c_k values are used to assess the applicability of each experiment to each design system. The E_{sum} and c_k values for four U(11)O₂ systems are presented in Table IV.

The trend plot of k_{eff} versus E_{sum} is given in Fig. 5 for the U(11)O₂ design system with H/X = 3. The bias and uncertainty in the bias is obtained from integral index trending by extrapolating the trending parameter to a value of 1.0. The slope of the trend curve is of secondary importance. The items of primary importance are the number of systems with high E_{sum} and c_k values and the value of the predicted Δk bias and uncertainty in the bias where $E_{sum} = 1.0$. The results from this trending analysis are shown in Table III. Figure 5 shows that few systems exhibit high E_{sum} values. Only 15 systems have E_{sum} values exceeding 0.5, and only one exceeds 0.8. A cutoff value for E_{sum} and c_k that can be used to determine applicability will be addressed later in this paper.

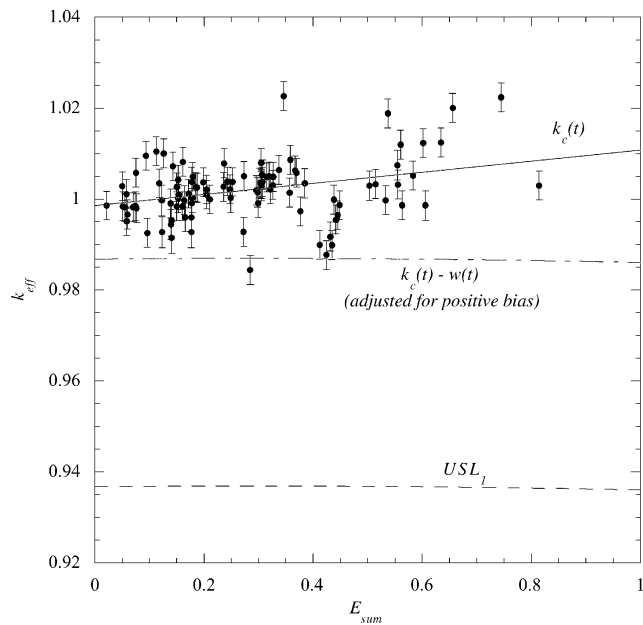


Fig. 5. Trend plot of k_{eff} versus E_{sum} for U(11)O₂ system with H/X = 3 for 100 benchmark experiments.

The trend plot of k_{eff} versus c_k for the U(11)O₂ system with H/X = 0 is shown in Fig. 6. This trend plot is interesting when compared with the traditional trend plot of k_{eff} versus EALF, shown in Fig. 3. The three data points in the upper-right portion of Fig. 6 correspond to three data points distributed across the top-middle portion of Fig. 3. The three corresponding systems are entries 44, 45, and 46 in Table II, the ZPR experiments. Each of these systems exhibits a c_k value in excess of 0.9 with this design system. As shown in Table III, the Δk bias β with the EALF trending is $\sim 0.18\%$. This bias is relatively small because the overprediction of k_{eff} for these four systems is counteracted by the underprediction of k_{eff} for entries 20 through 26 in Table II, six of the seven HEUMET experiments considered, which all have very similar values of EALF. However, the trending of k_{eff} with c_k , shown in Fig. 6, results in a Δk bias of 0.76%. The higher bias is caused by the lack of similarity between the U(11)O₂ H/X = 0 design system and the HEUMET systems. With this design system, these HEUMET systems have c_k values of ~ 0.4 to 0.6, indicating only minor correlations with the U(11)O₂ H/X = 0 system.

This example shows the potential improvement from the use of a traditional trending analysis with these new integral indices since trends can be observed as a function of systems that are expressly determined to be similar. The preceding analyses demonstrate that the traditional parameters can erroneously indicate that systems should be considered similar, where they are indeed different. Thus, using traditional techniques, it is necessary

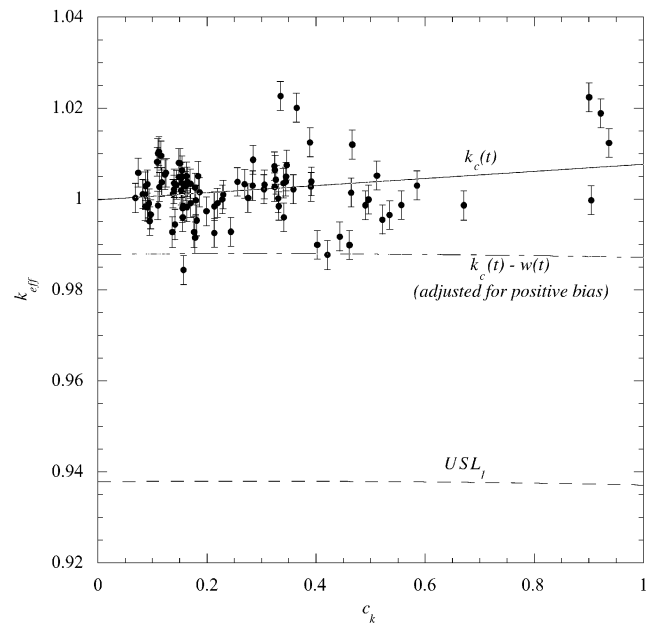


Fig. 6. Trend plot of k_{eff} versus c_k for U(11)O₂ system with H/X = 0 for 100 benchmark experiments.

TABLE IV

Integral Parameters for 100 Benchmark Experiments in Relation to Selected U(11)O₂ Design Systems

System Number	Identifier	c_k				E_{sum}			
		H/X = 0	H/X = 3	H/X = 40	H/X = 500	H/X = 0	H/X = 3	H/X = 40	H/X = 500
1	U(2)F4 - 195	0.3045	0.5604	0.8025	0.7063	0.0908	0.3220	0.8130	0.7840
2	U(2)F4 - 294	0.2558	0.4987	0.7897	0.7802	0.0614	0.2526	0.7878	0.8588
3	U(2)F4 - 406	0.2296	0.4555	0.7695	0.8272	0.0445	0.2048	0.7532	0.9043
4	U(2)F4 - 496	0.2193	0.4325	0.7529	0.8489	0.0363	0.1777	0.7239	0.9255
5	U(2)F4 - 614	0.2135	0.4117	0.7314	0.8637	0.0292	0.1500	0.6844	0.9423
6	U(2)F4 - 972	0.2138	0.3765	0.6700	0.8604	0.0180	0.0961	0.5683	0.9563
7	U(5)3O8 - 147	0.1990	0.5085	0.9084	0.8648	0.0879	0.3767	0.9214	0.8937
8	U(5)3O8 - 245	0.1570	0.4171	0.8428	0.9360	0.0522	0.2848	0.8645	0.9449
9	U(5)3O8 - 320	0.1508	0.3852	0.8070	0.9552	0.0386	0.2370	0.8231	0.9621
10	U(5)3O8 - 396	0.1393	0.3465	0.7627	0.9674	0.0306	0.2046	0.7864	0.9723
11	U(5)3O8 - 503	0.1375	0.3290	0.7392	0.9738	0.0232	0.1716	0.7421	0.9798
12	U(5)3O8 - 757	0.1401	0.3010	0.6862	0.9679	0.0142	0.1184	0.6456	0.9825
13	Godiva	0.4642	0.3734	0.1905	0.1091	0.5304	0.3570	0.0970	0.0058
14	Bapl-1	0.3232	0.5349	0.7633	0.7556	0.0817	0.2500	0.7493	0.8571
15	Bapl-2	0.2923	0.4959	0.7539	0.7991	0.0665	0.2120	0.7189	0.8893
16	Bapl-3	0.2627	0.4467	0.7237	0.8368	0.0500	0.1648	0.6617	0.9187
17	Big-10	0.9043	0.6047	0.0512	0.0008	0.8913	0.5329	0.1181	0.0074
18	HISS (HUG)	0.4663	0.7897	0.6505	0.2631	0.1692	0.5605	0.3747	0.0385
19	U(98) H ₂ O refl.	0.4960	0.4658	0.3240	0.2421	0.5259	0.4380	0.3929	0.2415
20	HEUMET A	0.4022	0.3695	0.2580	0.1141	0.5995	0.4120	0.1374	0.0091
21	HEUMET B	0.4208	0.3843	0.2619	0.1124	0.6210	0.4243	0.1383	0.0092
22	HEUMET C	0.4431	0.3995	0.2612	0.1110	0.6355	0.4318	0.1360	0.0091
23	HEUMET D	0.4613	0.4105	0.2574	0.1096	0.6430	0.4344	0.1300	0.0087
24	HEUMET E	0.5215	0.4488	0.2657	0.1079	0.6698	0.4423	0.1393	0.0097
25	HEUMET F	0.5347	0.4571	0.2654	0.1077	0.6750	0.4448	0.1395	0.0097
26	HEUMET G	0.5562	0.4704	0.2650	0.1076	0.6829	0.4488	0.1400	0.0097
27	HEUMET H	0.3351	0.2756	0.1491	0.0941	0.5431	0.3459	0.0742	0.0048
28	ORNL-1	0.0868	0.1594	0.5058	0.9214	0.0068	0.0515	0.4311	0.9537
29	ORNL-2	0.0910	0.1684	0.5183	0.9272	0.0074	0.0554	0.4554	0.9571
30	ORNL-3	0.0949	0.1765	0.5284	0.9305	0.0079	0.0584	0.4709	0.9534
31	ORNL-4	0.0967	0.1805	0.5332	0.9317	0.0082	0.0598	0.4768	0.9504
32	ORNL-10	0.1099	0.1710	0.4591	0.8454	0.0032	0.0216	0.3144	0.9375
33	PCTR 3.73	0.3583	0.4525	0.5050	0.5621	0.0838	0.2475	0.6538	0.7177
34	PCTR 3.78	0.3912	0.5584	0.6585	0.6013	0.0823	0.2434	0.6581	0.7328
35	PCTR 3.83	0.3907	0.5554	0.6538	0.6002	0.0800	0.2359	0.6497	0.7372
36	PCTR 5.84	0.3441	0.5026	0.6458	0.6658	0.0549	0.1777	0.6063	0.7982
37	PCTR 5.99	0.3451	0.5181	0.6750	0.6768	0.0545	0.1795	0.6130	0.7998
38	PCTR 6.23	0.3409	0.5029	0.6531	0.6737	0.0509	0.1657	0.5915	0.8086
39	PCTR 6.9	0.3318	0.5019	0.6709	0.6955	0.0476	0.1611	0.5942	0.8194
40	PCTR 6.95	0.3307	0.4910	0.6509	0.6881	0.0459	0.1524	0.5770	0.8231
41	PCTR 7.14	0.3267	0.4861	0.6498	0.6939	0.0453	0.1525	0.5801	0.8255
42	PCTR 7.52	0.3235	0.4824	0.6488	0.6979	0.0426	0.1434	0.5662	0.8330
43	PCTR 7.52a	0.3240	0.4923	0.6681	0.7062	0.0438	0.1507	0.5823	0.8307
44	ZPR 3/11	0.9218	0.6379	0.0933	0.0217	0.8942	0.5371	0.1195	0.0073
45	ZPR 3/12	0.9370	0.7712	0.2751	0.0974	0.9213	0.6020	0.1511	0.0099
46	ZPR 6/6a	0.9003	0.8867	0.4517	0.1978	0.9197	0.7450	0.2450	0.0264
47	UH3 NI	0.3643	0.5737	0.5378	0.2848	0.3994	0.6563	0.5444	0.3314
48	UH3 UR	0.5851	0.8324	0.7189	0.3303	0.5828	0.8145	0.6276	0.3258
49	TRX-1	0.3346	0.5535	0.7802	0.7512	0.0966	0.2784	0.7763	0.8619
50	TRX-2	0.2619	0.4521	0.7346	0.8365	0.0588	0.1819	0.6830	0.9224
51	ORNL L7	0.1252	0.3470	0.7631	0.8882	0.0710	0.3698	0.8522	0.9418
52	ORNL L8	0.0741	0.1537	0.5275	0.9489	0.0096	0.0750	0.5026	0.9634
53	ORNL L9	0.0872	0.1595	0.5048	0.9203	0.0066	0.0505	0.4270	0.9530

(Continued)

TABLE IV (Continued)

System Number	Identifier	c_k				E_{sum}			
		H/X = 0	H/X = 3	H/X = 40	H/X = 500	H/X = 0	H/X = 3	H/X = 40	H/X = 500
54	ORNL L10	0.0909	0.2684	0.6989	0.9345	0.0517	0.3052	0.8187	0.9615
55	ORNL L11	0.0825	0.1569	0.5108	0.9293	0.0078	0.0577	0.4481	0.9560
56	SHEBA	0.1536	0.3616	0.7689	0.9656	0.0357	0.2041	0.7913	0.9846
57	RF 0.77 A	0.6157	0.6126	0.4002	0.2205	0.6568	0.5641	0.3879	0.0924
58	RF 0.77 B	0.3485	0.6606	0.9388	0.7765	0.2010	0.5802	0.9553	0.8200
59	RF 0.77 C	0.3403	0.5844	0.8748	0.9030	0.1400	0.4129	0.8724	0.9414
60	RF 0.77 D	0.3788	0.7112	0.9614	0.7462	0.2372	0.6540	0.9745	0.7804
61	RF 2.03 A	0.3418	0.6622	0.9328	0.7541	0.1685	0.4936	0.9303	0.7880
62	RF 2.03 B	0.2882	0.5717	0.8948	0.8567	0.1206	0.3747	0.8702	0.8953
63	RF 2.03 C	0.5139	0.8106	0.9078	0.5918	0.3734	0.6766	0.9163	0.5844
64	RF 2.03 D	0.5000	0.8036	0.9118	0.5959	0.3496	0.6717	0.9266	0.5996
65	HST29-1	0.1230	0.3353	0.7547	0.9050	0.0509	0.3066	0.8495	0.9333
66	HST29-2	0.1480	0.3739	0.7799	0.8967	0.0510	0.3050	0.8541	0.9270
67	HST29-3	0.1530	0.3790	0.7808	0.8972	0.0504	0.2962	0.8491	0.9231
68	HST29-4	0.1701	0.4012	0.7918	0.8901	0.0525	0.2994	0.8476	0.9066
69	HST29-5	0.1695	0.4008	0.7925	0.8914	0.0556	0.3054	0.8527	0.9089
70	HST29-6	0.1626	0.3928	0.7901	0.8944	0.0584	0.3195	0.8634	0.9187
71	HST29-7	0.1541	0.3826	0.7858	0.8968	0.0594	0.3270	0.8689	0.9268
72	HST30-1	0.0688	0.1872	0.6057	0.9674	0.0226	0.1783	0.7261	0.9844
73	HST30-2	0.0869	0.2077	0.6148	0.9681	0.0189	0.1539	0.7049	0.9837
74	HST30-3	0.0939	0.2154	0.6160	0.9645	0.0161	0.1390	0.6883	0.9810
75	HST30-4	0.1543	0.4144	0.8129	0.8360	0.0564	0.3669	0.8688	0.8990
76	HST30-5	0.1443	0.3701	0.7796	0.8979	0.0563	0.3261	0.8660	0.9299
77	HST30-6	0.1485	0.3753	0.7817	0.8968	0.0542	0.3154	0.8607	0.9261
78	HST30-7	0.1634	0.3936	0.7897	0.8931	0.0538	0.3070	0.8549	0.9150
79	HST31-1	0.1537	0.3814	0.7833	0.8964	0.0526	0.3023	0.8531	0.9243
80	HST31-2	0.1840	0.4179	0.7947	0.8848	0.0500	0.2731	0.8262	0.8972
81	HST31-3	0.1608	0.3905	0.7878	0.8950	0.0548	0.3055	0.8530	0.9176
82	HST31-4	0.1867	0.4236	0.8005	0.8842	0.0595	0.2983	0.8387	0.8915
83	ICT02-1	0.1414	0.3072	0.6831	0.9430	0.0262	0.1393	0.6552	0.9646
84	ICT02-2	0.1366	0.3125	0.6968	0.9339	0.0327	0.1770	0.7426	0.9021
85	ICT02-3	0.1793	0.3541	0.6978	0.9205	0.0255	0.1225	0.6304	0.9577
86	ICT02-4	0.1809	0.3649	0.7148	0.9223	0.0288	0.1405	0.6857	0.9000
87	ICT02-5	0.1766	0.3515	0.6978	0.9227	0.0255	0.1233	0.6275	0.9545
88	ICT02-6	0.1782	0.3622	0.7145	0.9243	0.0287	0.1407	0.6789	0.8949
89	LCT32-1	0.2838	0.6259	0.9533	0.7899	0.1534	0.5033	0.9611	0.8358
90	LCT32-2	0.2691	0.5881	0.8740	0.7030	0.1571	0.5147	0.9538	0.7801
91	LCT32-3	0.3054	0.6446	0.9175	0.6993	0.1789	0.5558	0.9616	0.7331
92	LCT32-4	0.1090	0.2595	0.6593	0.9605	0.0301	0.1618	0.7010	0.9797
93	LCT32-5	0.1131	0.2732	0.6749	0.9568	0.0346	0.1844	0.7548	0.9218
94	LCT32-6	0.1170	0.2866	0.6911	0.9554	0.0377	0.1986	0.7776	0.8960
95	LCT32-7	0.1159	0.2263	0.5815	0.9288	0.0180	0.0938	0.5495	0.9652
96	LCT32-8	0.1120	0.2297	0.5963	0.9364	0.0209	0.1128	0.6226	0.9121
97	LCT32-9	0.1100	0.2343	0.6088	0.9418	0.0231	0.1261	0.6548	0.8861
98	LST05-1	0.1550	0.2775	0.5700	0.8232	0.0129	0.0766	0.5395	0.9741
99	LST05-2	0.1565	0.2787	0.5691	0.8211	0.0124	0.0741	0.5316	0.9716
100	LST05-3	0.1632	0.2834	0.5612	0.8039	0.0117	0.0699	0.5209	0.9669

to produce a tailored set of benchmarks to trend against, while S/U techniques can be used with large-multiple-system-type benchmark datasets.

The trend plots for the remaining U(11)O₂ systems with H/X values of 3, 40, and 500 are presented in Figs. 7,

8, and 9, with the values of the β , $\Delta\beta$, and USL₁ presented in Table III. For the system with an H/X value of 3, the predicted biases are higher than those predicted by the standard techniques. The specific reasons for these differences were not explored in depth as with the H/X

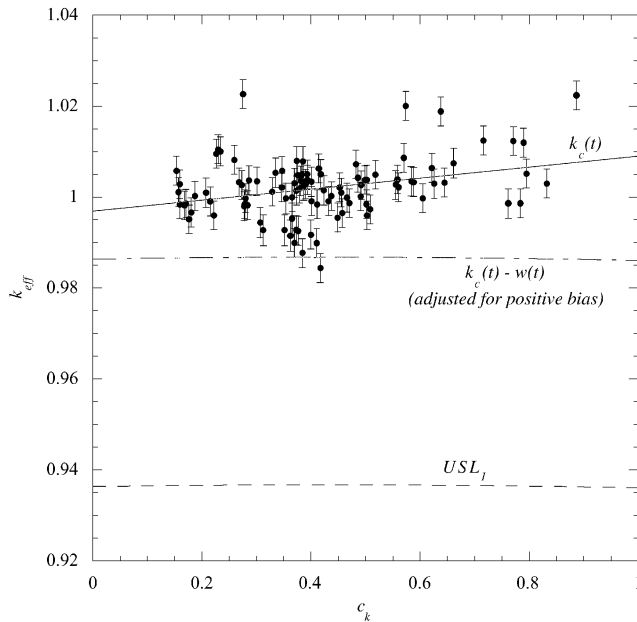


Fig. 7. Trend plot of k_{eff} versus c_k for U(11)O₂ system with H/X = 3 for 100 benchmark experiments.

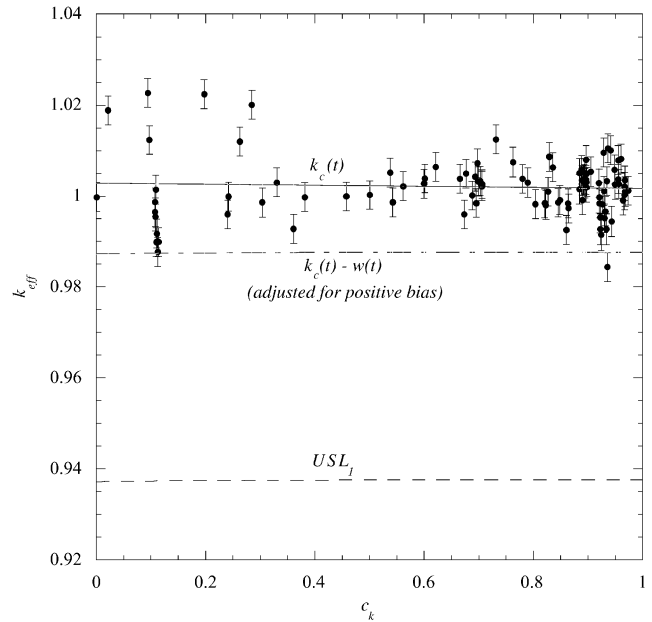


Fig. 9. Trend plot of k_{eff} versus c_k for U(11)O₂ system with H/X = 500 for 100 benchmark experiments.

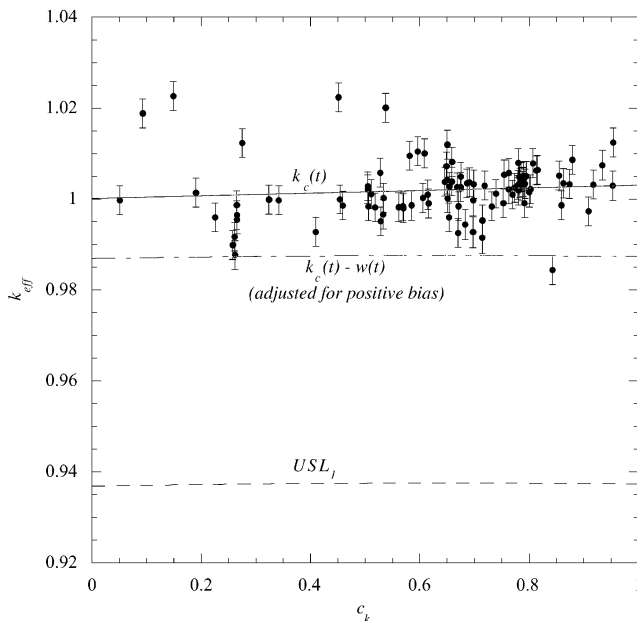


Fig. 8. Trend plot of k_{eff} versus c_k for U(11)O₂ system with H/X = 40 for 100 benchmark experiments.

of 0 cases but are believed to be caused by the separation of effects that tended to cancel each other in trending with traditional parameters. In any case, it should be noted that in this instance, experiments with higher c_k values generally have calculated k_{eff} values that are ≥ 1 . The Δk biases predicted for the H/X = 40 and H/X =

500 systems with the c_k trending are consistent with those predicted with traditional techniques since there are a large number of experiments considered to be similar, and no cancellation of effects is observed.

A comparison of the c_k versus E_{sum} integral indices for four selected U(11)O₂ systems is shown in Fig. 10. This plot demonstrates a general 1:1 correlation of c_k with E_{sum} , with the exceptions of the design systems with H/X = 3 and H/X = 500 for values of c_k below 0.9. For the H/X = 3 systems, the E_{sum} values are lower than the c_k values. Further investigation revealed that this effect is caused by the intermediate-energy spectrum of the U(11)O₂ H/X = 3 system. Few experiments examined here have similar energy spectra, leading to lower E_{sum} values. However, the cross-section–uncertainty data in this energy range, particularly in the ²³⁵U capture and fission cross sections, increase the overall correlations in the uncertainties for the various systems, and hence, the c_k values are large relative to the E_{sum} values.

The opposite effect is seen for the H/X = 500 system. Here, the E_{sum} values generally exceed the c_k values. In the H/X = 500 design system, the importance of the ¹H scattering reaction, as assessed by the magnitude of the energy-integrated sensitivity coefficients, exceeds the importance of ¹H scattering in the H/X = 3 system by a factor of 5. The energy-integrated ¹H scattering sensitivity coefficients are 0.5521 and 0.0995 for the H/X = 500 and H/X = 3 systems, respectively. Additionally, the cross-section data for ¹H scattering is relatively well known with small tabulated uncertainties. Experiments with thermal energy spectra exhibit similar

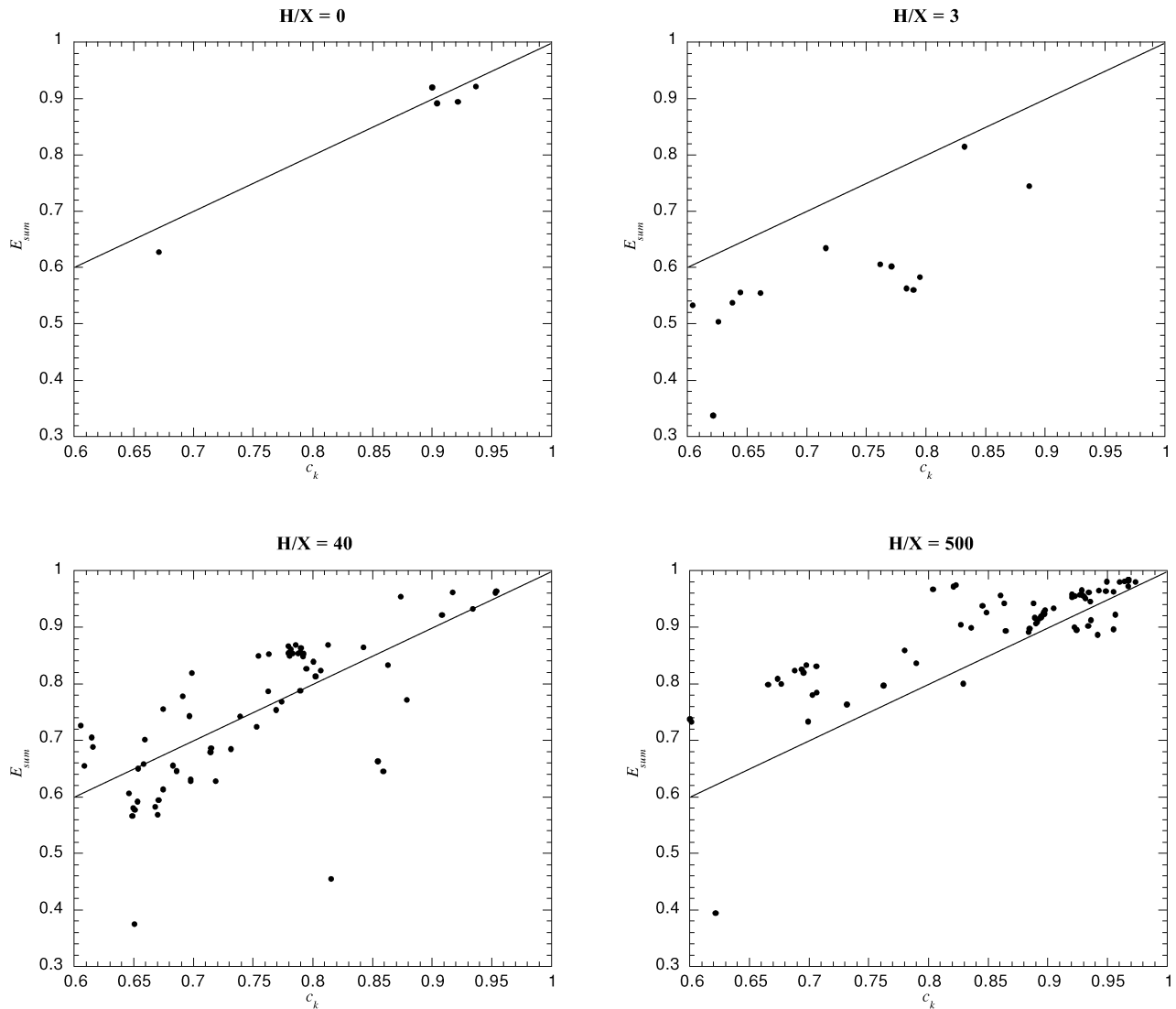


Fig. 10. E_{sum} versus c_k values for four $U(11)O_2$ applications: $H/X = 0, 3, 40,$ and 500 .

sensitivities to 1H scattering as the $H/X = 500$ design system. These similarities in an important nuclide-reaction pair can lead to high-valued E_{sum} parameters. However, the small-valued uncertainty data minimize the impact of the similar sensitivity coefficients in the calculation of c_k . Although the experiments do indeed provide excellent coverage for 1H scattering for this system, a nuclide-reaction pair with small cross-section-data uncertainties is not believed to make a significant contribution to the computational bias. Thus, the reduced value of c_k , relative to E_{sum} , indicates that other important nuclide-reaction pairs with higher cross-section-data uncertainties may not be covered as well by the experiments.

As a comparison of the use of c_k or E_{sum} for establishing applicability of experiments for use in code val-

idation calculations, the numbers of systems exceeding a value of 0.8 for c_k and E_{sum} is shown in Table V. The choice of 0.8 is somewhat arbitrary, but a c_k value of 0.8 represents that 80% of the variance, due to data uncertainties, in the design system is shared by the experimental benchmark. An E_{sum} value of 0.8 represents that 80% of the sensitivity of k_{eff} to its constituent cross-section data is common to the two systems.

Table V also contains the number of systems with $T(E) > 0.95$ for the major nuclide-reaction pairs for each of these four application areas. The 0.95 criterion indicates similarity between the energy-dependent sensitivity of k_{eff} to a particular nuclide-reaction pair in the benchmark system and the design system. The use of $T(E)$ allows the determination of reaction-specific applicability of the benchmark. The acceptance criterion of

TABLE V
Number of 100 Benchmark Systems Matching Selected Criterion for U(11)O₂ Systems

Criterion	H/X = 0	H/X = 3	H/X = 40	H/X = 500
$c_k > 0.8$	4	2	16	58
$E_{sum} > 0.8$	4	1	31	70
$T(E) > 0.95$ -H capture	—	—	83	24
$T(E) > 0.95$ -H scatter	—	6	51 ^a	48 ^a
$T(E) > 0.95$ -O scatter	0	0	3	27
$T(E) > 0.95$ - ²³⁵ U fission	2 ^a	2 ^a	4 ^a	49 ^a
$T(E) > 0.95$ - ²³⁵ U capture	15	4	25	30
$T(E) > 0.95$ - ²³⁸ U fission	6 ^a	2 ^a	4	—
$T(E) > 0.95$ - ²³⁸ U capture	0 ^a	0 ^a	6 ^a	40 ^a

^aTop three sensitivities.

0.95 is preliminary and based only on heuristic arguments. However, a comparison of the global acceptance criteria and the reaction-specific criteria is interesting.

The global similarity criteria require the major sensitivity components of each system pair to match; however, the reaction-specific criteria require only the individual cross-section processes to match. The reaction-specific tests do not consider whether or not the process is important in the system, only that the sensitivity of the benchmark to the selected process is greater than that for the design system. The numbers of systems, shown in Table V, meeting the reaction-specific criterion for the nuclide-reaction pairs with the highest sensitivities are generally less than the numbers meeting the global-based criteria. This discrepancy in the numbers of systems meeting each criterion indicates that $T(E) > 0.95$ is a more stringent criterion than the $E_{sum} > 0.80$ criterion. Preliminary work has suggested that a criterion of $T(E) > 0.90$ might be more appropriate. Further work is required for the establishment of better guidance on appropriate limits for these integral indices.

VII.D. GLLSM Analysis

The GLLSM procedure was applied to determine the computational bias and its uncertainty for the U(11)O₂ systems in reference to the same set of 100 benchmark experiments used in the previous trending analyses. For this analysis, the data input to GLLSM included the sensitivity data and computed value of k_{eff} for each benchmark experiment and each design system, the experimentally measured value of k_{eff} and its reported uncertainty for each benchmark experiment, and the cross-section-covariance data. For experiments without reported experimental uncertainties, a uniform value of 0.3% was used. The GLLSM procedure allows for the use of correlated uncertainties within the experimental data. However, this option was not used in this analysis. Although this option is not used in the current analysis, an exam-

ple application of the χ^2 -consistency indicator is presented in Ref. 25.

The GLLSM procedure produced an adjusted set of cross-section data to minimize the difference between the measured and computed values of k_{eff} . The effect of the data adjustment on the computed value of k_{eff} for each design system was realized by propagating the adjustment to k_{eff} via the sensitivity coefficients. The difference between the computed k_{eff} value of the design system with the standard data and with adjusted cross sections represents the computational bias. The predicted computational bias β and the uncertainty in k_{eff} are shown in TABLE III. Here, the uncertainty is not in the bias and does not represent a confidence band as is presented for the other procedures. Rather, for each design system, the value presented as $\Delta\beta$ is the uncertainty in the computed k_{eff} (percent standard deviation), due to cross-section data uncertainties, for the adjusted set of cross-section data. This value is somewhat analogous to the pooled standard deviation s_p in Eq. (4). Thus, a value analogous to USL_1 is not available from this procedure for comparison with the other procedures. The computational bias β predicted by GLLSM does have the same interpretation as that predicted by the other procedures.

Because the GLLSM procedure predicts the computational bias through a data adjustment technique, the benchmark experiments used to produce the adjustments have a great impact on the results of the analysis. Because the k_{eff} covariance matrix \mathbf{C}_{kk} , is explicitly included in the GLLSM adjustment procedure and in the calculation of the c_k values, c_k provides a measure of the appropriateness of the benchmark experiment for use in the data adjustment procedure. With the inclusion of more experiments with higher c_k values, the data adjustment, and thus the computational bias predicted by GLLSM, becomes more reliable. For the U(11)O₂ systems, as shown in Table V, very few benchmarks exhibit $c_k \geq 0.8$ for the H/X = 0 and H/X = 3 systems. Because of the lack of experiments that are highly correlated to these

design systems, the GLLSM does not have enough information to produce a reliable estimate of the computational bias.

VIII. ESTABLISHMENT OF APPLICABILITY CRITERIA

The relationship between GLLSM and c_k can be used to determine a criterion for c_k that indicates whether or not a design system falls within the area of applicability of the benchmark experiment. For this exercise, repetitive GLLSM calculations were carried out for five of the $U(2)F_4$ systems in the benchmarking set, entries 1 through 5 in Table II, with H/X values ranging from 195 to 614. Because these are actual critical experiments, the computational bias for each system is known. The intent of this exercise was to determine the magnitude of the c_k value necessary to obtain convergence of the GLLSM procedure. It is expected that with sufficient information, GLLSM should converge to an adjusted data set that minimizes the difference in the experimental and calculated k_{eff} values. For each of the first five entries in Table II, the c_k values for each of the 100 experiments from Table II were computed. For each of the five systems, the GLLSM analysis was repeated by removing

the experiments with the highest c_k values from the analysis in increments of 0.01. Thus, the first GLLSM analysis included all 100 experiments, even the system for which the bias was to be minimized, which by definition has a c_k value of 1.0. The next analysis included only experiments with c_k values of 0.99 and lower, then 0.98 and lower, and so forth. The results of this exercise are shown in Fig. 11. The horizontal axis of Fig. 11 presents the cutoff for c_k used in the calculation. The vertical axis presents the bias β_a obtained from Eq. (44). The value of the bias should not exceed the stated uncertainty in the experimental measurements when the system itself is included in the GLLSM analysis. The endpoints of the data shown in Fig. 11 do not deviate from a zero bias by more than the experimental uncertainty.

The values of β_a , with decreasing c_k , are fairly constant for the first several data points of each curve plotted in Fig. 11. In all cases the β_a value is nearly constant to the point of removing experiments with c_k values of 0.9 and higher. When including only the experiments with c_k values of 0.89 and lower, the value of y for the H/X = 195 system begins a dramatic change. Similar changes are observed at c_k values of 0.86, 0.82, 0.80, and 0.78 for systems with H/X values of 294, 406, 496, and 614, respectively. Even though these results correspond only to $U(2)F_4$ systems, these clear breaks in the

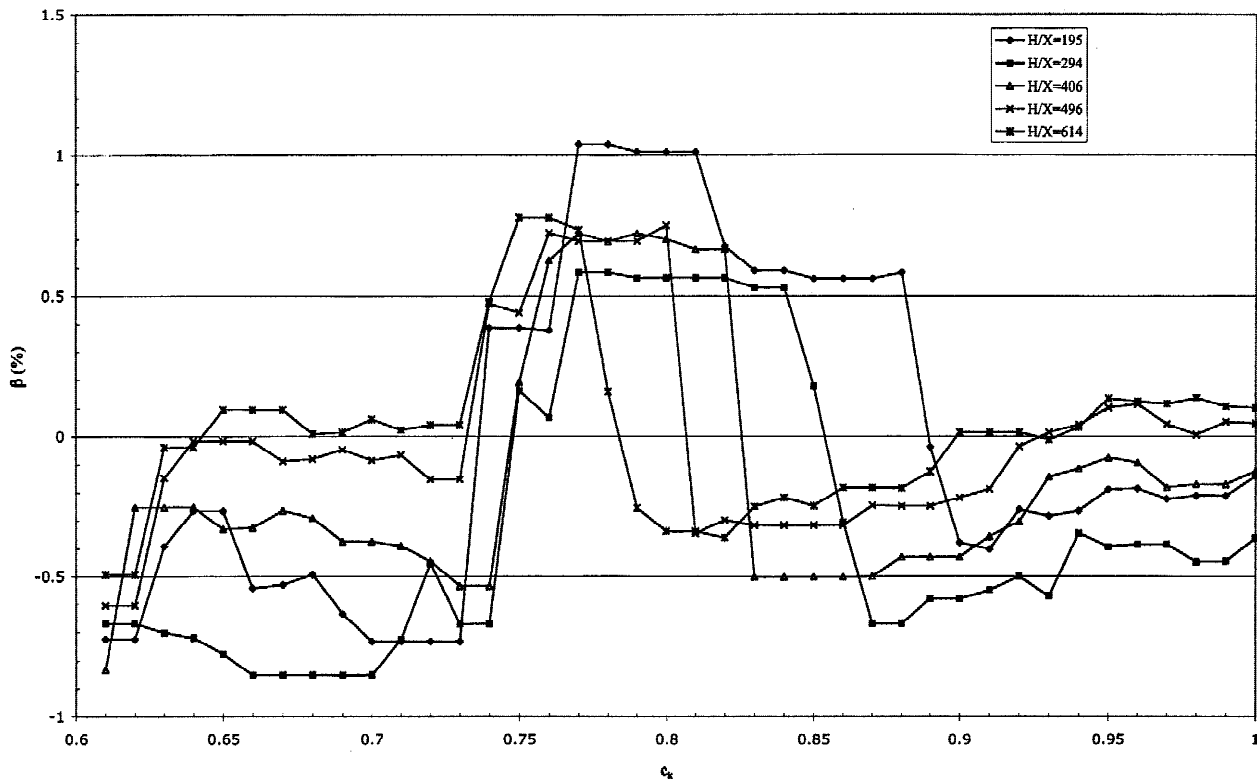


Fig. 11. Dependence of GLLSM predicted bias on the inclusion of only experiments with correlation coefficients of less than c_k for $U(2)F_4$ systems.

behavior of the data adjustment produced by the GLLSM procedure indicate that a design system falls within the area of applicability of experiments with c_k values of 0.9 and greater and may fall within the area of applicability of experiments with c_k values as low as 0.78. The applicability criterion of $c_k \geq 0.8$, as recommended in Ref. 16, is not unreasonable but should be used with caution. In this example, the applicability criteria demonstrated an inverse correlation with H/X; however, it is not known if this is a general trend for all areas of applicability. The applicability criteria will be studied further in continuing work on this subject.

The number of correlated systems necessary to obtain convergence of the GLLSM procedure was also investigated. For each of the U(2)F₄ systems, benchmark experiments were incrementally included in the analysis beginning with experiments exhibiting c_k values of 0.90 to 0.91. Next, experiments exhibiting c_k values of 0.90 to 0.92 were included, then 0.90 to 0.93, and so forth. Convergence of the procedure was determined where the value of y agreed within 1σ of the endpoint value. In this case, the standard deviation used was the propagated adjusted cross-section uncertainty determined by the diagonal elements of $\mathbf{C}_{k'k'}$ computed in Eq. (45). For the five series of calculations, a range of 14 to 22 systems was required for convergence of the GLLSM procedure. This convergence procedure is illustrated in Fig. 12, where

the error bars on the endpoints represent 1σ . When repeating this analysis by incrementally including systems with c_k values of 0.80 and higher, 25 to 40 systems were required to obtain convergence within 1σ . Based on these results, an adequate assessment of the computational bias and its uncertainty for a design system can be determined with a suite of approximately 15 to 20 benchmark experiments that demonstrate c_k values of 0.9 or higher. These guidelines are more stringent than those given in Ref. 16, which recommends 5 to 10 benchmarks with c_k values of 0.9 or higher and 15 to 20 benchmarks with c_k values of 0.8 or higher. Additionally, the currently proposed criteria are based on the evaluation of the thermal systems. In an earlier evaluation of fast HEU and Pu metallic spheres, the data adjustments of the GLLSM procedure were found to converge with as few as four systems that were very similar in spectra and material composition.²² Because of the similarity of c_k and E_{sum} , the same limits developed for c_k should also be applicable to the use of the E_{sum} parameter.

IX. SUMMARY

This paper has presented the theoretical basis for the application of S/U analysis methods to the validation of

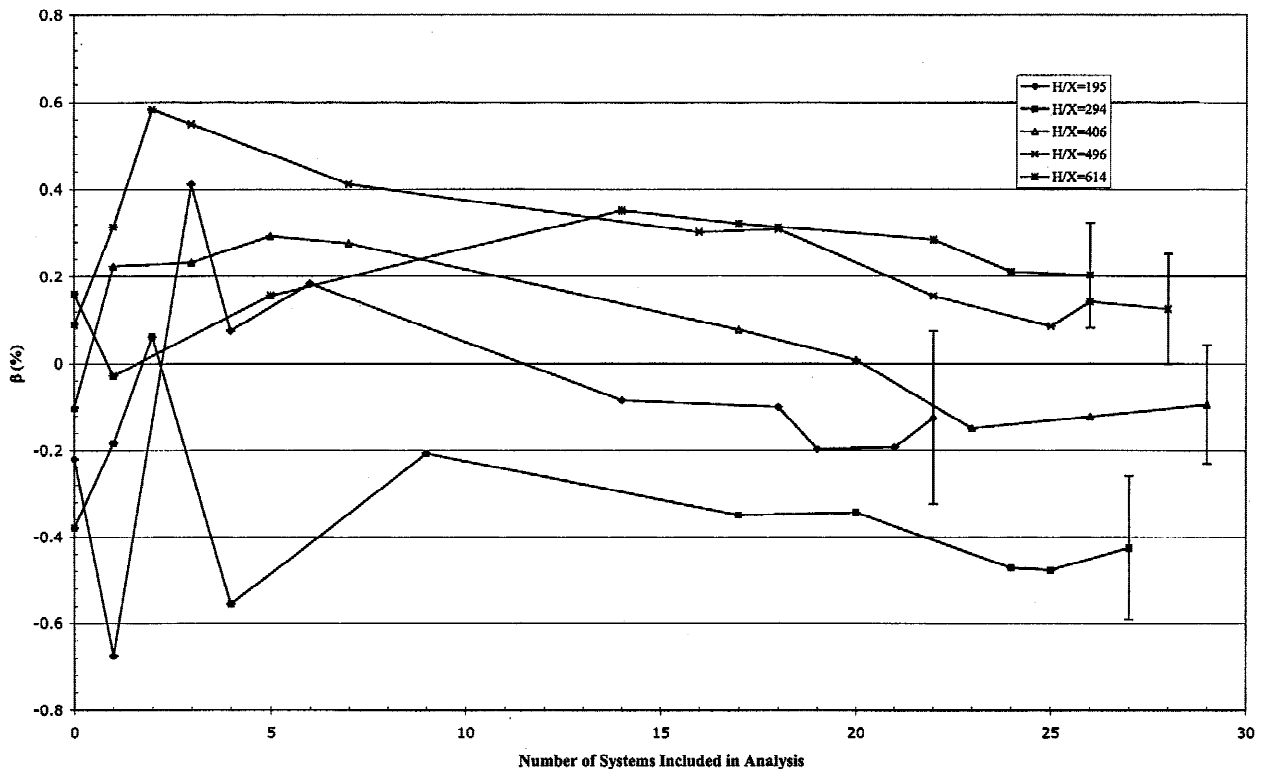


Fig. 12. Convergence of GLLSM predicted bias with inclusion of experiments with $c_k > 0.9$ for U(2)F₄ systems.

data sets for use in criticality safety applications and compared their use to the methods traditionally employed in validation of criticality safety analysis methods. The new validation techniques involve updated S/U analyses, similar to those developed in the late 1970s primarily for use in the development of fast reactor systems. The sensitivity analyses produce energy-dependent sensitivity values (sensitivity profiles), which give the relative change in the system k_{eff} value as a function of relative changes in the cross sections by energy. These analyses provide the basic understanding of the physics of each benchmark experiment in order to properly characterize similarities between systems in a consistent manner. The uncertainty analyses provide an estimate of the uncertainties in the calculated values of the system k_{eff} due to cross-section uncertainties, as well as correlations in the k_{eff} uncertainties between systems. The use of both sensitivity and S/U analyses in the formal determination of areas of applicability has been developed in this work. These determinations of applicability can be accomplished via integral indices, which represent the similarity in the sensitivity profile values and/or the correlation coefficients c_k . Ranges of these indices, proposed to formally define the applicability of a series of critical benchmark experiments to a particular application area, are c_k and E_{sum} values that are 0.90 or higher. These indices relate directly to the similarity between pairs of systems. This similarity can be used to establish the applicability of a benchmark experiment to the criticality code validation of a design system.

The elements used in the S/U analysis, along with the calculated and measured k_{eff} values and estimates of uncertainties in the measurements, were used in this work to demonstrate application of the GLLSM procedure to data validation for criticality safety studies. The primary goal of the GLLSM analysis is the prediction of the calculated-versus-measured differences for systems that have not been measured. These calculated-versus-measured differences are the so-called computational biases. Application of the GLLSM procedures to a series of critical experiments is designed to identify "changes" in the underlying nuclear data such that the calculated-versus-measured differences are minimized. This work has identified the relationship between these predicted data changes and the computational bias for systems that have not been measured and hence correspond to interpolations or extrapolations in the vector space corresponding to the original set of benchmark experiments. Uncertainties in the bias can be estimated based on the standard deviation provided by the GLLSM procedure.

A benchmark database of 100 experiments, which included not only computational models and measured-versus-computational k_{eff} results but also S/U results generated by the S/U methodology, was developed. The same tools were then applied to a set of four application scenarios corresponding to U(11)O₂ systems with H/X val-

ues ranging from 0 to 500. An area of applicability determination was performed using the c_k and E_{sum} integral indices generated in the S/U analysis. The analysis indicated that the benchmark dataset had good coverage of the 11 wt% systems with H/X values >40, while the systems with H/X values <40 had only marginal-to-inadequate coverage. The scarcity of low-H/X benchmark experiments is a concern. Additional experiments in this area would be useful.

Additionally, analyses were performed to predict the computational biases for the 11 wt% systems. Specifically, the traditional k_{eff} trending analyses were compared with newly developed k_{eff} trending procedures, utilizing the c_k and E_{sum} parameters, as well as the GLLSM procedure.

Comparisons of the various trending techniques were quite interesting in that the differences in the biases predicted by the various methods depend on the particular system being analyzed. The predicted biases for various systems were in some cases up to a factor of 5 differences between the various trending parameters. The primary reason for these differences is that systems demonstrating similarity from the standpoint of certain parameters may be dissimilar with respect to other parameters. In particular, the H/X and EALF parameters predicted similarity between dry uranium systems with high enrichments (93 wt%) and dry uranium systems with intermediate enrichments (10 wt%), while the c_k and E_{sum} indices indicated that these systems were quite different. The net effect of trending with H/X and EALF was a cancellation of the effects of the biases on the trend, which produced a predicted design system bias of <0.5% overprediction for a dry U(11)O₂ system. The trending with c_k and E_{sum} integral indices produced an estimated bias of nearly 1% overprediction since a number of systems predicted to be very similar to the dry U(11)O₂ system demonstrated an overprediction calculated value of k_{eff} . Although the predicted biases from these applications are all positive, and thus not considered in the calculation of the USL, the differences in magnitude are a concern since the prudent application of trending procedures is very important in criticality safety analysis validation exercises.

The example application given herein is included primarily for illustrative purposes. Further study is ongoing with the aim of providing specific guidance on the application of these techniques to criticality safety validation studies.

Studies have indicated that 15 to 20 benchmarks with c_k values near or exceeding 0.9 are needed to ensure convergence in a GLLSM procedure. Therefore, a corresponding number and type of systems should be considered a minimum to establish the area of applicability covering the design system. Under certain conditions, convergence can also be expected for 25 to 40 systems with c_k values >0.8. The type of conditions under which convergence can be produced with systems with c_k values

<0.9 is the subject of current research. This work has shown that the c_k and E_{sum} values perform equally well for the set of applications considered. Hence, the same criterion used for the c_k values should be applicable to the E_{sum} values. Additional studies will be performed to verify this observation.

Future work in this area of study may involve determining procedures to be followed if a sufficient number of benchmarks experiments with integral indices equal to 0.9 cannot be identified and addressing the issue of cross-section data for which no uncertainty data are available.

ACKNOWLEDGMENTS

The authors acknowledge the technical contributions of R. L. Childs, formerly of ORNL. The authors further acknowledge the support and encouragement of this work by C. Nilsen and D. Damon of the U.S. Nuclear Regulatory Commission (NRC) and H. Johnson, J. McKamy, and J. Felty of the U.S. Department of Energy (DOE). The work described in this paper was funded by support from the NRC and the DOE Nuclear Criticality Safety Program.

Oak Ridge National Laboratory is managed and operated by UT-Battelle, LLC, for the U.S. Department of Energy under contract DE-AC05-00OR22725.

REFERENCES

1. "Nuclear Criticality Safety in Operations with Fissionable Materials Outside Reactors," ANSI/ANS-8.1-1998, American Nuclear Society (1998).
2. J. J. LICHTENWALTER, S. M. BOWMAN, M. D. DEHART, and C. M. HOPPER, "Criticality Benchmark Guide for Light-Water-Reactor Fuel in Transportation and Storage Packages," NUREG/CR-6361 (ORNL/TM-13211), U.S. Nuclear Regulatory Commission/Oak Ridge National Laboratory (1997).
3. R. K. DISNEY, "A Review of the Current State-of-the-Art Methodology for Handling Bias and Uncertainty in Performing Criticality Safety Evaluations," INEL-94/0251, UC-501, Idaho National Engineering Laboratory (1994).
4. "SCALE: A Modular Code System for Performing Standardized Computer Analysis for Licensing and Evaluations," NUREG/CR-0200, Rev. 6 (ORNL/NUREG/CSD-2/R6), Vols. I, II, and III, CCC-545, Radiation Safety Information Computational Center (May 2000).
5. R. L. CHILDS, "SEN1: A One-Dimensional Cross-Section Sensitivity and Uncertainty Module for Criticality Safety Analysis," NUREG/CR-5719 (ORNL/TM-13738), U.S. Nuclear Regulatory Commission/Oak Ridge National Laboratory (1999).
6. B. T. REARDEN, "Perturbation Theory Eigenvalue Sensitivity Analysis with Monte Carlo Techniques," *Nucl. Sci. Eng.*, **145**, XXX (2004).
7. American National Standard for Criticality Safety Criteria for the Handling, Storage, and Transportation of LWR Fuel Outside Reactors, ANSI/ANS-8.17-1984 (R 1997), American Nuclear Society (1997).
8. H. R. DYER and C. V. PARKS, "Recommendations for Preparing the Criticality Safety Evaluation of Transport Packages," NUREG/CR-5661 (ORNL/TM-11936), U.S. Nuclear Regulatory Commission/Oak Ridge National Laboratory (1997).
9. E. M. OBLOW, "Sensitivity Theory from a Differential Viewpoint," *Nucl. Sci. Eng.*, **59**, 187 (1976).
10. W. M. STACEY, Jr., "Variational Estimates and Generalized Perturbation Theory for the Ratios of Linear and Bilinear Functionals," *J. Math. Phys.*, **13**, 1119 (1972); see also W. M. STACEY, Jr., "Variational Estimates of Reactivity Worths and Reaction Rate Ratios in Critical Nuclear Reactors," *Nucl. Sci. Eng.*, **48**, 444 (1972).
11. L. N. USACHEV, "Perturbation Theory for the Breeding Ratio and for Other Number Ratios Pertaining to Various Reactor Processes," *J. Nucl. Energy* **18**, parts A/B, 571 (1964).
12. A. GANDINI, "A Generalized Perturbation Method for Bilinear Functionals of the Real and Adjoint Neutron Fluxes," *J. Nucl. Energy*, **21**, 755 (1967).
13. C. R. WEISBIN, J. H. MARABLE, J. L. LUCIUS, E. M. OBLOW, F. R. MYNATT, R. W. PEELLE, and F. G. PEREY, "Application of FORSS Sensitivity and Uncertainty Methodology to Fast Reactor Benchmark Analysis," ORNL/TM-5563, Oak Ridge National Laboratory (Dec. 1976); see also "Application of Sensitivity and Uncertainty Methodology to Fast Reactor Integral Experiment Analysis," *Nucl. Sci. Eng.*, **66**, 307 (1978).
14. M. L. WILLIAMS, B. L. BROADHEAD, and C. V. PARKS, "Eigenvalue Sensitivity Theory for Resonance-Shielded Cross Sections," *Nucl. Sci. Eng.*, **138**, 177 (2001).
15. *International Handbook of Evaluated Criticality Safety Benchmark Experiments*, NEA/NSC/DOC(95)03, Nuclear Energy Agency Nuclear Science Committee of the Organization for Economic Cooperation and Development (1999).
16. B. L. BROADHEAD, C. M. HOPPER, R. L. CHILDS, and C. V. PARKS, "Sensitivity and Uncertainty Analyses Applied to Criticality Safety Validation," NUREG/CR-6655, Vols. 1 and 2 (ORNL/TM-13692/V1 and V2), U.S. Nuclear Regulatory Commission/Oak Ridge National Laboratory (1999).
17. S. GOLOUGLU, C. M. HOPPER, and B. T. REARDEN, "Extended Interpretation of Sensitivity Data for Benchmark Areas of Applicability," *Trans. Am. Nuc. Soc.*, **88**, 77 (2003).

18. G. PALMIOTTI and M. SALVATORES, "Use of Integral Experiments in the Assessment of Large Liquid-Metal Fast Breeder Reactor Basic Design Parameters," *Nucl. Sci. Eng.*, **87**, 333 (1984).
19. J. D. SMITH III and B. L. BROADHEAD, "Multigroup Covariance Matrices for Fast Reactor Studies," ORNL/TM-7389, Oak Ridge National Laboratory (1981).
20. R. E. McFARLANE, R. J. BARRETT, D. W. MUIR, and R. M. BOICOURT, "The NJOY Nuclear Data Processing System: User's Manual," LA-7584-M, Los Alamos National Laboratory (1978).
21. M. E. DUNN, "PUFF-III: A Code for Processing ENDF Uncertainty Data into Multigroup Covariance Matrices," ORNL/TM-1999/235 (NUREG/CR-6650), U.S. Nuclear Regulatory Commission/Oak Ridge National Laboratory (2000).
22. A. PAZY, G. RAKAVY, I. REISS, J. J. WAGSCHAL, A. YA'ARI, and Y. YEIVIN, "The Role of Integral Data in Neutron Cross-Section Evaluation," *Nucl. Sci. Eng.*, **55**, 280 (1974).
23. R. L. PEREL, J. J. WAGSCHAL, and Y. YEIVIN, "PV-Surveillance Dosimetry and Adjustment: Review of Several Significant Oral Laws," in "Reactor Dosimetry: Radiation Metrology and Assessment," J. G. WILLIAMS, D. W. VAHAR, F. H. RUDDY, and D. M. GILLIAM, Eds., ASTM STP 1398, p. 486, American Society for Testing and Materials (2001).
24. J. D. SMITH III, "Processing ENDF/B-V Uncertainty into Multigroup Covariance Matrices," ORNL/TM-7221, Oak Ridge National Laboratory (1980).
25. B. L. BROADHEAD, C. M. HOPPER, S. C. FRANKLE, J. F. BRIESMEISTER, R. C. LITTLE, and J. J. WAGSCHAL, "Further Investigations of NIST Water Sphere Discrepancies," ORNL/TM-2000/173, Oak Ridge National Laboratory (2000).